A Szilikátipari Tudományos Egyesület lapja

építőanyag

Journal of Silicate Based and Composite Materials

A TARTALOMBÓL:

2019/1

EuCIA
European Composites Industry Association

COMPOSITES: NO LIMITS TO YOUR IMAGINATION

Imagine a lightweight, strong and durable material which can be manufactured in complex shapes in a cost-effective way. Imagine that its properties can be tailor-made by choosing a proper combination of components and layup sequences. Would you like to take the opportunity and unleash your imagination to design innovative solutions for a new challenging technical problem?

www.eucia.eu

építőanyag
Journal of Silicate Based and Composite Materials
2019/1

TARTALOM

CONTENT

A finomkerámia-, üveg-, cement-, mész-, beton-, tégla- és cserép-, kő- és kavics-, tűzállóanyag-, szigetelőanyag-iparágak szakmai lapja
Scientific journal of ceramics, glass, cement, concrete, clay products, stone and gravel, insulating and fireproof materials and composites

A folyóiratot referálja · The journal is referred by:
Cambridge Scientific Abstracts
ProQuest

A folyóiratban lektorált cikkek jelennek meg.
All published papers are peer-reviewed.
Kiadó · Publisher: Szilikátipari Tudományos Egyesület (SZTE)
Elnök · President: ASZTALOS István
1034 Budapest, Bécsi út 122–124.
Tel.: +36-1/201-9360 ▪ E-mail: epitoanyag@szte.org.hu
Tördelő szerkesztő · Layout editor: NÉMETH Hajnalka

Címlapfotó · Cover photo: GYURKÓ Zoltán

WWW.EPITOANYAG.ORG.HU
EN.EPITOANYAG.ORG.HU

Online ISSN: 2064-4477
Print ISSN: 0013-970x
INDEX: 2 52 50 ▪ 71 (2019) 1–32

Vol. 71, No. 1

Modeling of nonlinear viscoelastic polymeric materials at their large periodic deformation

N. A. CHERPAKOVA ▪ Altai State University, Russia ▪ nadja-cherpakova@mail.ru
G. V. PYSHNOGRAI ▪ Altai State University, Russia ▪ pyshnograi@mail.ru
P. FILIP ▪ Institute of Hydrodynamics, Academy of Sciences of Czech Republic ▪ filip@ih.cas.cz
R. PIVOKONSKY ▪ Institute of Hydrodynamics, Academy of Sciences of Czech Republic ▪ pivokonsky@ih.cas.cz

Érkezett: 2018. 07. 24. ▪ Received: 24. 07. 2018. ▪ https://doi.org/10.14382/epitoanyag-jsbcm.2019.1

Abstract

Analyzing the behavior of flows of polymers solutions and melts in the area of non-linear viscoelasticity allows to estimate more precisely the adequacy of the rheological model and to describe the material structure in more detail. Today a lot of models describe non-linear properties of polymeric materials rather accurately. However, the formulation of a uniform rheological model remains open. Therefore this work considers the modified Vinogradov-Pokrovsky rheological model which formed the basis for numerical calculations for periodic deformation of shear flows of polymeric liquids with a large amplitude. The non-linear viscoelastic properties shown in the course of the research of behavior of polymeric material at large deformations were studied by means of the immediate analysis of time dependence of shear stresses which were calculated at various amplitudes. It was stated that when increasing the amplitude of deformation the response stops being the exact harmonica, and a "step" on the left-hand front appears. It manifests the nonlinear response of a sample. The work compares obtained theoretical dependences and the experimental data for 5% mass solutions of the polyethylene oxide in dimethylsulfoxide which was studied at harmonic deformations with the large amplitude reaching 40 relative units. These dependences were measured at 35 °C and the frequency of 0.2 Hz. Despite its simplicity, the modified Vinogradov-Pokrovsky rheological model shows good compliance with the experimental data. The results show that the chosen model adequately describes behavior of polymeric materials at large periodic deformations. Therefore this model may be applied for modeling more complex flows of fluid polymeric environments.

Keywords: rheology, rheological model, non-linear viscoelasticity, oscillations, shear, polymers solutions
Kulcsszavak: reológia, reológiai modell, nemlineáris viszkoelaszticitás, oszcilláció, nyírás, polimer oldatok

N. A. CHERPAKOVA
graduate student of the Altai State University, Barnaul, Russia, Area of scientific interests: rheology, polymer melt, mesoscopic theory.

G. V. PYSHNOGRAI
Doctor of Physical and Mathematical Sciences, Professor, of Altai State University, Barnaul, Russia, Area of scientific interests: rheology, polymer melt, mesoscopic theory.

P. FILIP
Professor Technology of Macromolecular Substances. The Institute of Hydrodynamics of the Czech Academy of Sciences, Prague, Czech Republic. Research activities – Rheology.

R. PIVOKONSKY
Professor researcher, The Institute of Hydrodynamics of the Czech Academy of Sciences, Prague, Czech Republic. Research activities – Rheology.

1. Introduction

A number of rheological models [1-4] are often applied to describe rheological features of polymeric materials at quite small periodic or stationary deformations. However, when processing solutions and melts of polymers we have to face with deformation of higher orders. Therefore, practical reasons and more precise methods of measurements e.g. at larger periodic deformations [5-7] cause the transition from analyzing the behavior of flows in the linear viscoelastic area to studying non-linear effects. It promises a more reliable assessment of prognostic properties of some rheological models as their applicability for different types of deformation is extended. Therefore now modeling rheological features in the non-linear viscoelastic area is getting more and more popular. In fact, the measurements at large periodic deformations allow to describe the material structure in more detail [6].

Nowadays there are a lot of rheological models some of which are still developing whereas others have already lost their relevance. The most prominent are: Gizekus model [1], Leonov-Prokunin model [2], the extended pom-pom model [3], the modified Vinogradov-Pokrovsky (mVP) model [4]. All of them describe well the linear effects at small periodic deformations and non-linear effects at large stationary deformations. Recently the new research has appeared and now it is developing rapidly. It studies the rheological behavior of polymeric liquids developed at periodic oscillations with a large amplitude [5]. This work will study the structural change of the material response while the amplitude of deformation increases. Primarily the work aims at checking the adequacy of the mVP rheological model.

As [6] shows, non-linear viscoelastic features which are observed when studying the behavior of polymeric material at large deformations may be interpreted via Lissajous figures or analyzing time dependencies of shear stresses obtained at various deformations. Thus the increase in oscillation amplitude means increase in nonlinearity of the sample response.

2. Mathematical model

The numeric calculations are based on the equations written down on the basis of the mVP rheological model [4]. The model is unique since it considers the tensor nature of the friction coefficient for beads which is defined by the induced anisotropy of a shift flow. The model looks as following:

$$\sigma_{ik} = -p\delta_{ik} + 3\frac{\eta_0}{\tau_0}a_{ik};$$
$$\frac{d}{dt}a_{ik} - v_{ij}a_{jk} - v_{kj}a_{ji} + \frac{1+(\kappa-\beta)I}{\tau_0}a_{ik} = \frac{2}{3}\gamma_{ik} - 3\frac{\beta}{\tau_0}a_{ij}a_{jk}. \quad (1)$$

Here σ_{ik} – a stress tensor; p – hydrostatic pressure; η_o and τ_0 – initial values of shear viscosity and relaxation time for a polymeric component; v_{ik} – velocity gradients tensor; a_{ik} – the symmetric second rank tensor of anisotropy; $I = a_{jj}$ – first invariant of anisotropy tensor; $\gamma_{ik} = (v_{ik} + v_{ki})/2$ - symmetrized tensor of velocity gradients; κ, β – phenomenological parameters of the model considering the sizes and the form of a macromolecular ball in macromolecule dynamical equations and which are connected by a ratio: $\kappa=1.2\cdot\beta$, that corresponds with condition of independence of asymptotical behavior of stationary shear viscosity of the polymer molecular weight [4].

Based on Eq. (1) modeling of oscillations was carried out, both with large and small amplitudes. The polymeric sample is supposed to have been exposed to deformations with frequency ω under the harmonic law with the given amplitude γ_0: $\gamma(t) = \gamma_0 \sin(\varpi t)$. In this case only one component of velocity gradients tensor v_{ij} is different from zero: $v_{12}(t)=\gamma_0\varpi\cos(\varpi t)$. The material response represents the tension-to-time dependence. According to the calculations, the periodic mode of oscillations is set quite rapidly in a polymeric system at deformation from immobility ($\sigma_{ik}(0)=0$).

At the small amplitude shear stresses arising in the material are directly proportional to deformation that is they represent the exact harmonica. At periodic deformation of the material with the larger amplitude the response stops being the exact harmonica. The results of modeling (*Fig. 1*) and experiments [5] both confirm that.

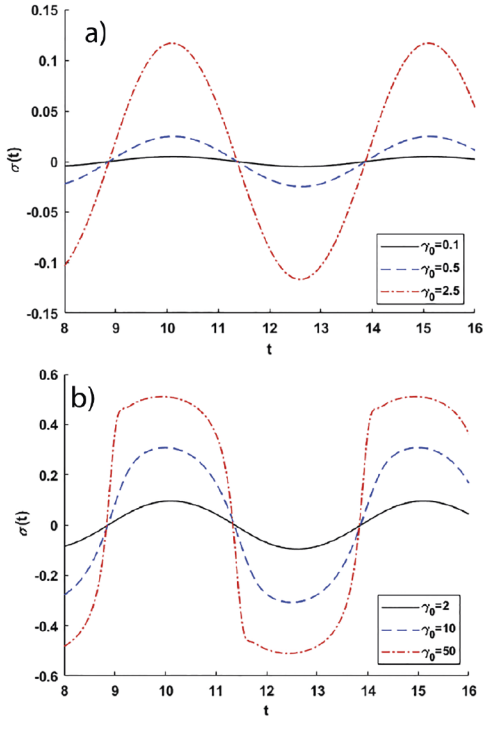

Fig. 1. Change of a response of material at increase in amplitude of deformation of material a) – small amplitudes; b) – large amplitudes)
1. ábra Anyag válaszának függése a deformáció amplitúdójától a) kis amplitúdók; b) nagy amplitúdók

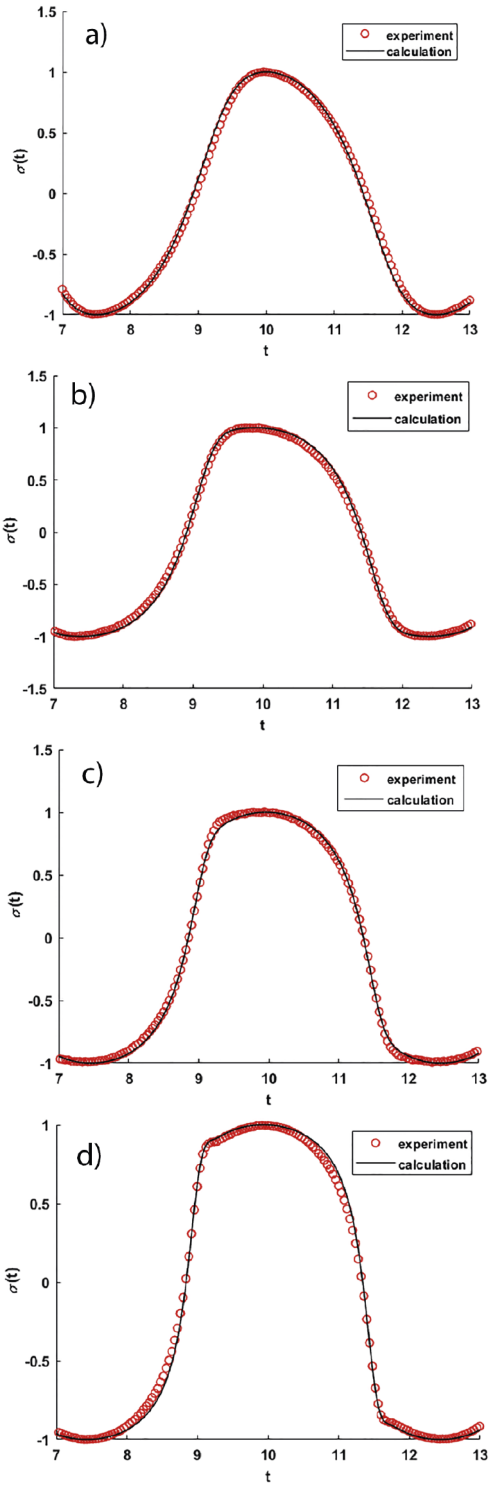

Fig. 2. Comparison of theoretical dependence and the experimental data for the normalized shear stresses σ(t) in the set mode with various relative amplitudes of deformation a) – 5; b) – 10; c) – 20; d) – 40)
2. ábra Normalizált nyírófeszültség σ(t) összehasonlítása elméleti összefüggések és mért adatok között a) – 5; b) – 10; c) – 20; d) – 40)

3. Comparing modeling results and the experiment

A large number of works, referred to in [5-7], is devoted to a research of transient and stationary rheological features at large periodic deformations. In the experimental data [7] the 5%

mass solution of polyethylene oxide in a dimethylsulfoxide was exposed to deformation. The polymeric solution was exposed to harmonic deformation at large amplitude γ_0, sequentially reaching values of 50%, 100%, 500%, 1000%, 2000% and 4000% at frequency ω = 0.2 Hz.

The application of the mVP rheological model was checked for efficiency by optimizing model parameters κ=0.045; β=0.038; τ_0=0.21 sec; η_0= 87.3534 Pas·s. in the linear area (at small periodic deformations). Further the behavior of the model with the found parameters was compared to the results of experiments at large periodic deformations.

Fig. 2 shows the comparison of the established dependences of the normalized response calculated via the Runge-Kutta method with the experimental data from [7].

It is noticeable that the left and right fronts of oscillations are deformed differently at increased relative amplitude. The graph of experimental dependences shows the emergence of a step at the increased amplitude. At increased γ_0 the right front deviates from harmonica without a step. The model describes this effect rather precisely (*Fig. 2*). The comparisons between the obtained results and previous experimental data mean that the model provides for a quite precise description of polymeric materials at large periodic deformations.

4. Conclusions

The work provided for modeling a non-linear viscoelasticity of the polymeric material at its large periodic deformations via the mVP model. The results were compared with the experimental data of 5% mass solution of polyethylene oxide in dimethylsulfoxide which was studied at harmonic deformations of large amplitude reaching 40 relative units measured at 35°C and the frequency of 0.2 Hz [5].

Nonlinearity of the studied sample manifests itself in the response distortion for the material as it stops being the exact harmonica. The considered model allows to model the non-linear effects arising at increased amplitude of material deformation. It is also possible to use this model for modeling more complex flows of fluid polymeric media.

It is curious that such a simple model as Eq. (1) which considers only one relaxation process complies so greatly to the experimental data. When describing the non-linear dependence of shift viscosity and normal stresses of the first-order difference, this model shows only qualitative compliance of calculated dependences and the experimental data [4,8,9].

Further research plans to modify the considered model for a multimode case in order to increase the accuracy of the results. Also the model will be studied via the Lissajous figures.

Acknowledgments

One of the authors (CheNA) acknowledgment financial support of the Russian Foundation for Basic Research (RFBR) under grant 18-31-00030.

The authors (P.F. and R.P.) wish to acknowledge the Grant Agency CR for the financial support of Grant Project No. 17-26808S and the Institutional Research Plan RVO 67985874.

References

[1] Giesekus, H. (1982): A simple constitutive equation for polymer fluids based on the concept of deformation-dependent tensorial mobility. *Journal of Non-Newtonial Fluid Mechanics*, 1982. Vol. 11. pp. 69–109. https://doi.org/10.1016/0377-0257(82)85016-7

[2] Leonov, A. I. (1992): Analysis of simple constitutive equations for viscoelastic liquids. *Journal of Non-Newtonial Fluid Mechanics*, 1992. Vol. 42. pp. 323–350. https://doi.org/10.1016/0377-0257(92)87017-6

[3] Pivokonsky, R. – Filip, P. (2014): Predictive/fitting capabilities of differential constitutive models for polymer melts —reduction of nonlinear parameters in the eXtended Pom–Pom model. *Colloid and Polymer Science*, 2014. 292. pp. 2753–2763. https://doi.org/10.1007/s00396-014-3308-7

[4] Merzlikina, D. A. – Pyshnograi, G. V. – Pivokonskii, R. – Filip P. (2016): Rheological model for describing viscometric flows of melts of branched polymers. *Journal of Engineering Physics and Thermophysics*, Vol. 89, No. 3, May, 2016, pp. 652–659. https://doi.org/10.1007/s10891-016-1423-7

[5] Ilyin, S. O. – Malkin, A. Ya. – Kulichikhin, V. G. (2014): Application of large amplitude oscillatory shear for the analysis of polymer material properties in the nonlinear mechanical behavior. *Polymer Science Series A*, 2014. V.56. pp. 98-110. https://doi.org/10.1134/S0965545X14010039

[6] Ewoldt, R. H. – Hosoi, A. E. – McKinley, G. H (2008): New measures for characterizing nonlinear viscoelasticity in large amplitude oscillatory shear. *Journal of Rheology*, Vol. 52, No. 6. https://doi.org/10.1122/1.2970095

[7] Pivokonsky, R. – Filip, P. – Zelenkova, J. (2017): Two Ways to Examine Differential Constitutive Equations: Initiated on Steady or Initiated on Unsteady (LAOS) Shear Characteristics. *Polymers*. 2017. V.9. pp 205 https://doi.org/10.3390/polym9060205

[8] Koshelev, K. B. – Pyshnograi, G. V. – Tolstykh, M. Y. (2015): Modeling of the three-dimensional flow of polymer melt in a convergent channel of rectangular cross-section. *Fluid Dynamics*. 2015. Vol. 50. No. 3. pp 315-321. https://doi.org/10.1134/S0015462815030011

[9] Pyshnograi, G. V. – Gusev, A. S. – Pokrovskii, V. N. (2009): Constitutive equations for weakly entangled linear polymers. *Journal of Non-Newtonian Fluid Mechanics*. 2009. V. 164. No. 1-3. pp 17-28. https://doi.org/10.1016/j.jnnfm.2009.07.003

Ref.:
Cherpakova, N. A. – **Pyshnograi**, G. V. – **Filip**, P. – **Pivokonsky**, R.: *Modeling of nonlinear viscoelastic polymeric materials at their large periodic deformation*
Építőanyag – Journal of Silicate Based and Composite Materials, Vol. 71, No. 1 (2019), 2–4. p.
https://doi.org/10.14382/epitoanyag-jsbcm.2019.1

Modified clay for the synthesis of clay-based nanocomposites

David P. PENALOZA Jr.
Associate professor in the Chemistry Department, College of Science, De La Salle University. His research interests focus on self-assembled systems and nanostructured materials.

David P. PENALOZA Jr. ▪ Chemistry Department, College of Science, De La Salle University, Manila ▪ david.penaloza.jr@dlsu.edu.ph

Érkezett: 2018. 08. 12. ▪ Received: 12. 08. 2018. ▪ https://doi.org/10.14382/epitoanyag-jsbcm.2019.2

Abstract

This review article highlights usual surface modification methodologies in clay fillers for polymer nanocomposites. In clay-based polymer nanocomposites preparation, a key step is the homogeneous dispersion and random orientation of the silicate platelets, like that of montmorillonite (MMT), in the polymer matrix resulting in an exfoliated nanohybrid materials, where significant works in the literature support enhanced and/or new properties of the resulting nanocomposites compared to the bare polymer. In incorporating the MMT clay as a filler in a polymeric material, the surface modification of an MMT clay is necessary. An MMT clay is made up of layered silicates carrying negative charges held together by metal cations found in the galleries between the clay layers. If left unmodified, the native clay exists as aggregates. To improve its miscibility toward organic molecules, it is necessary to modify the clay fillers for polymer nanocomposites.

Keywords: Silicate clay, clay modification, montmorillonite, organoclay
Kulcsszavak: Szilikátos agyag, agyag modifikálás, montmorillonit, szerves agyag

1. Introduction

A polymer-clay nanocomposite represents a new class of hybrid materials composed of an organic polymer matrix with an inorganic clay acting as a filler material having at least one dimension in the nanometer range. A fully exfoliated, individual clay platelet is about a nanometer in thickness. At this length scale, the presence of these individual nanometer thin platelets dispersed in the polymer matrix even at a low amount of the silicate filler (<10% by wt) can impact the resulting hybrid organic-inorganic material to exhibit greatly enhanced and new properties relative to the neat polymer [1-9]. These new and enhanced properties observed for these nanomaterials have found numerous applications and have attracted the attention of both the academe and the industries. The homogeneous dispersion of these nanometer-sized silicate platelets within a polymer matrix can lead to the formation of a hybrid material that exhibits markedly improved properties such as higher modulus, increased thermal stability and flame retardancy, and more efficient gas barrier properties, as compared to their unfilled polymers or conventional composites counterparts.

Among the clay fillers, the montmorillonite (MMT) clay is the usual choice in preparing most polymer-clay nanocomposites because of its individual nanometer-thick platelets, extremely large surface areas, rich intercalation and surface chemistry [10-12]. Further, this type of clay is universally abundant in nature and can be obtained in pure form at a low cost.

An MMT clay, being hydrophilic in nature, obviously would only be miscible with hydrophilic polymers like poly(ethylene oxide), poly(vinyl alcohol), etc. Generally, it would be very difficult to mix this clay with hydrophobic polymers because of its pristine hydrophilic nature. If left unmodified, it would be very difficult to achieve a homogeneous of clay and polymer where the clay filler is randomly well distributed in the hydrophobic polymer matrix [13]. In any nanocomposite preparation, one major challenge is the achievement of a high degree of exfoliation of the aluminosilicate layered structure to yield well-dispersed individual clay platelets in the nanocomposite. This type of morphology for the clay is the target of most modification techniques since the exfoliation of the clay fillers creates a bulk material of interfaces as opposed to the intercalation or agglomeration of the layered silicates in the composite material [14-16]. Hence, modifying the clay filler prior to its incorporation in various polymeric matrices has been usually observed.

2. Montmorillonite clay

Montmorillonite (MMT) clay is a naturally-occurring hydrous aluminum silicate clay belonging to a class of clay known as 2:1 phyllosilicates. The clays belonging to this class are commonly regarded as layered silicates [17]. Other layered silicate clays aside from MMT clay include vermiculite, saponite and hectorite (*Table 1*). The MMT clay has a layered morphology consisting of stacks of silicate platelets that are about 1-nm thick and about 300 nm to a few microns in lateral dimensions. Each individual platelet has a central octahedral sheet of alumina fused between two external silica tetrahedral sheets (*Fig. 1*). The tetrahedral sheet is mainly composed of silica while the octahedral sheet is comprised of diverse elements like Al, Mg and Fe [18]. The stacking of the layers leads to a regular *van der Waals* gap called the interlayer or gallery. Isomorphic substitution (for example, Al^{3+} replaced by Mg^{2+} or Fe^{2+}) within the layers generates negative charges that are counterbalanced by cations residing in the interlayers (*Fig. 2*). In their pristine form, their excess negative charge is balanced by cations (Na^{+}, Li^{+}, Ca^{2+}) which exist hydrated in the interlayers. The cations are held very loosely and can be readily exchanged by other cations.

Layered clay	Formula	CEC (meq/ 100 g clay)
Hectorite	$M_x(Mg_{6-x}Li_x)Si_8O_{20}(OH)_4$	120
Montmorillonite	$M_x(Al_{4-x}Mg_x)Si_8O_{20}(OH)_4$	92.6-120
Saponite	$M_xMg_6(Si_{8-x}Al_x)Si_8O_{20}(OH)_4$	86.6
Vermiculite	$(Mg, Fe, Al)_3[(Al, Si)_4O_{10}](OH)_2M_{x^*}nH_2O$	150

***M** represents the exchangeable cations found in the interlayer of the clays and **x** refers to the layer charge*

Table 1 Charge exchange capacities (CEC) of some 2:1 phyllosilicates
1. táblázat Töltés cserekapacitások (CEC) egyes 2:1 filoszilikátokra

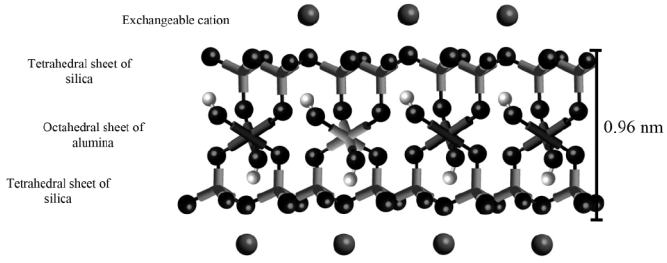

Fig. 1. An individual montmorillonite clay platelet is about a nanometer thick and is composed of an octahedral sheet of alumina sandwiched by two tetrahedral sheets of silica. Isomorphic substitution (for example, Al^{3+} replaced by Mg^{2+} or Fe^{2+}) within the layers generates negative charges that are counterbalanced by cations residing in the interlayers.
1. ábra Egy kb. 1 nanométer vastagságú montmorillonit lemez, amely egy oktaéderes aluminát lemezből áll közrefogva két tetraéderes szilikát lemezzel. A lemezek közötti izomorf helyettesítés (pl. Al^{3+} ion helyettesítése Mg^{2+} vagy Fe^{2+}ionokkal) negatív töltést generál,amelyet a lemezközi kationok kompenzálnak.

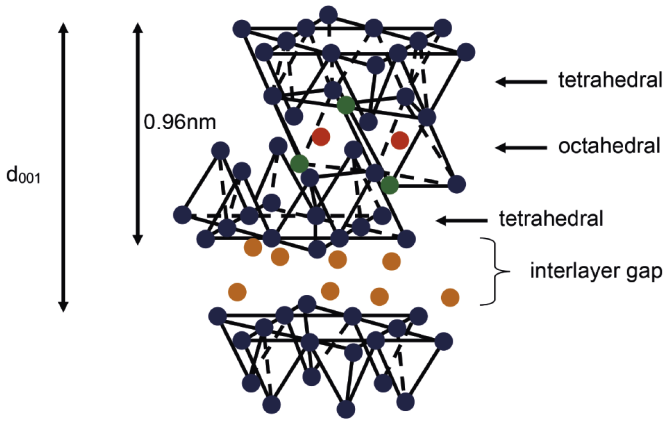

Fig. 2. The stacking of the silicate platelets (each about a nanometer thick) leads to a regular van der Waals gap called the interlayer or gallery. Inside the galleries, highly exchangeable cations are found. Replacement of these ions by alkyl surfactants can lead to the increased distance of the interlayer gaps.
2. ábra A szilikát lemezek kapcsolódása szabályos van der Waals rést eredményez (rétegközi galéria). A galériákon belül erős cserepotenciálú kationok találhatók. Ezek cseréje alkil felületaktív gyökökkel a rétegközi réstávolság növekedéséhez vezet.

There are two attractive features why an MMT clay is commonly exploited in the preparation of polymer-clay nanocomposites. The MMT clay has highly exchangeable ions that are found at the interlayers. These cations can be easily substituted with organic surfactants, i.e. the use of ion exchange reaction. For example, the reaction between an alkyl ammonium salt and the MMT clay results in the replacement of these cations with alkyl chains that increase the interlayer gaps as well as change the surface chemistry of the MMT clay. Also, the MMT clay has high aspect ratio (100 - 1000) that can be maximized through the dispersion of the individual silicate layers in a polymer continuum. These two characteristics are, of course, interrelated because the ability to disperse the silicate layers in a polymer matrix, thereby maximizing their aspect ratio, depends on the chemical nature of the interlayer cation.

At a low filler loading, usually less than 10 wt.%, the reinforcement efficiency of exfoliated silicate platelets as fillers to form polymer-clay nanocomposites can match that of a conventional composite that is usually made using a relatively higher loading (40–50 wt.%) of classical fillers. This improvement is due to the dispersion of the nanoscale fillers into the matrix, which results in a high surface area with high interactions between the nanoclay and the polymer matrix [19-21].

3. Clay modification

In preparing clay-based polymer nanocomposites, a homogeneous dispersion and random orientation of the silicate platelets of the clay filler in the polymer matrix is desired for a fully exfoliated system. Another consideration is the favorable interaction between the polymer and the clay filler in order to avoid phase separation and agglomeration of the filler particles in the polymer matrix. In incorporating the MMT clay as a filler in a polymeric material, the surface modification of an MMT clay is necessary. An MMT clay is made up of layered silicates carrying negative charges held together by metal cations found in the galleries between the clay layers. The presence of metal cations and the ability of forming hydrogen bonds with water contribute to the hydrophilic nature of the pristine MMT. Hence, pristine MMT clay is difficult to mix with an organic matrix especially if it involves hydrophobic polymers. If left unmodified, the native clay exists as aggregates. To improve its miscibility toward organic molecules, it is necessary to modify the surface chemistry of the MMT clay. One method of modification is the replacement of the inorganic cations found in the interlayers with various organic cationic molecules. The intercalation of organic molecules in the clay galleries can lead to the increased interlayer spacing. This surface treatment also makes the clay to become more compatible with polymer molecules. The increased interlayer gap and the favorable interaction posed by the alkyl intercalants found in the clay galleries of the organoclay allow the polymer molecules to enter the enlarged basal spacing of the organoclay for further intercalation and which may eventually lead to the clay exfoliation.

3.1 Clay modification via ion-exchange reaction

To make the hydrophilic clay more compatible with the polymer matrix, surface modification techniques have been commonly employed on clays used as fillers prior to their incorporation in the polymers. An ion exchange reaction between the MMT clay and an ammonium-based alkyl salt as an intercalant [22-26] is one. The clay surface can be converted from being hydrophilic to organophilic via a cation exchange reaction with an alkyl ammonium ion that may include a primary, secondary, tertiary or quaternary alkyl ammonium

salt. The change in surface property of the clay brought about by an ion exchange reaction can improve the interfacial adhesion properties between the inorganic phase (clay filler) and the organic phase (polymer matrix) when a hydrophobic polymer matrix is involved [27]. The alkyl intercalant of the modified clay can also increase the interlayer distance of the silicate layers where the increase in the basal spacing is affected by the length of the alkyl chain and the ratio of cross-sectional area to available area per cation [28]. Long-chain alkyl ammonium-exchanged forms of MMT are the most commonly used in the preparation of most clay-based polymer systems. Quaternary ammonium salts, of the general formula $[NR_4]^+X^-$ where R is a hydrocarbon chain and X is a halide group, have been commonly employed in the organophilic modification of MMT via an ion exchange reaction [29-31]. This is possible due to the presence of highly exchangeable metal ions residing in the galleries of pristine MMT clays. On the addition of the alkyl ammonium salt to the aqueous clay suspension, the long alkyl cations replace the metal ions originally present in the clay galleries. The ammonium groups become ionically anchored to the negative clay surface with the long hydrocarbon chains radiating away from the clay surface. The intercalation of the organic surfactant not only changes the surface property of the clay (making it more hydrophobic) but also increases the basal spacing of the clay layered structure which favors the intercalation of long polymer molecules.

Depending on the chain length and charge density of the clay, the alkyl chains can adopt several conformations inside the clay galleries. *Lagaly* (1986) [32] proposed that the alkyl ammonium ions used to modify 2:1 clay minerals lie either parallel to the silicate surface forming mono- or bilayers or radiate away from the surface forming paraffin-type arrangement. The organic intercalant may adopt a monolayer, quasi-bilayer or multi-layer configuration based on the length of the alkyl chain [27, 33-36].

Vaia and his co-reresearchers (1994) [36] studied the structure of an organoclay of MMT, modified with dioctadecyl dimethyl ammonium, $(CH_3(CH_2)_{16}CH_2)_2N^+(CH_3)_2$, by X-ray diffraction (XRD), infrared spectroscopy (IR), and differential scanning calorimetry (DSC) and showed that the alkyl chains assume an ordered state. That is, the alkyl ammonium cations build a self-assembled monolayer (SAM) on the mineral surface. The authors postulated that the arrangements of the alkyl chains in the clay interlayer vary from solid-like to liquid-like and in intermediate cases, liquid crystalline, depend on the packing density and chain length (*Fig. 3*). An ordered state for the alkyl chains intercalated in the clay can be observed at a particular length and number of chains due to the increasing chain interactions and the packing density of the tethered chains. At this stage, the chains attached to the platelets are proposed to interdigitate [27]. In the interdigitated arrangement of the tethered alkyl ammonium ions, their conformational entropy is minimized while the packing density of the attached chains is maximized. The authors also proposed that in their ordered state, the alkyl chains inside the MMT galleries preferentially assume an all-trans conformation with the alkyl chains tilted to the MMT surface at an angle (*Fig. 3.c*) [27, 34-35].

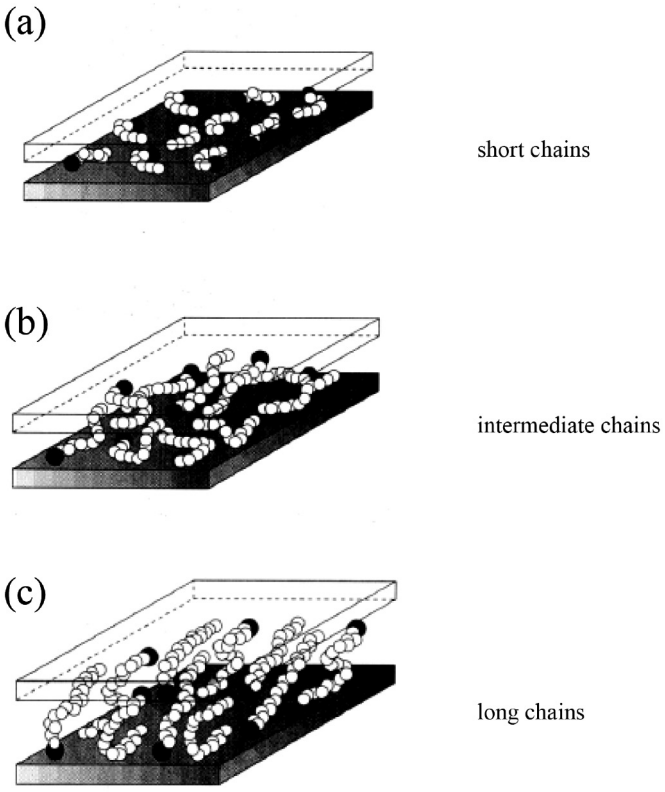

Fig. 3. Possible conformation of alkyl chains of an ammonium-based intercalant in the interlayer gaps of an organo-modified montmorillonite clay as a function of chain length: (a) short chains; (b) intermediate chains forming a quasi-bilayer; and (c) long chains with increased order and multi-layer spacing [36]

3. ábra Ammónium alapú felületaktív alkil láncok lehetséges kapcsolódási formái montmorillonit agyaggal a lánchossz függvényében (a) rövid láncok; (b) közepes láncok kvázi-bíréteg formációval; (c) hosszú láncok magasabb rendezettséggel és többrétegű formációval [36]

The organo-modified clays were found to self-assemble parallel to each other inside the clay galleries forming alternating, well-ordered organic/inorganic multi-layers based on molecular dynamic (MD) simulations. *Hackett* and co-workers (1998) [37] used MD simulations to study the static and dynamic properties of 2:1 layered silicates (CEC = 0.8, 1.0 and 1.5 meq/g for two MMT clays and a hectorite, respectively) that are modified with ammonium-based alkyl surfactants. The MD simulations they conducted for these organoclays showed that the basal spacing increased with the length of the alkyl chain of the onium salts used as a modifier. The results further showed that within the gallery, the alkyl chains exhibit layering tendencies. The shorter alkyl chains form a monolayer configuration with an interlayer gap of 1.3 nm. As these chains become longer, bilayer (d_{001}=1.8 nm) and trilayer (d_{001}=2.27 nm) disordered arrangements can be observed.

Okutomo et al. (1999) used various silylating agents having different chain lengths to react with a magadiite clay previously ion exchanged with an alkyl ammonium modifier (C_{12}TMA-magadiite). They reported that an increase in the number of carbon in the alkyl chain corresponds to a larger basal spacing of the resulting organoclay. After silylation, the basal spacing changed from 2.79 nm (before silylation) to 1.95, 2.33 and 3.25 nm for the C_{42}C1Si$^-$, C_{82}C1Si$^-$ and C_{182}C1Si$^-$-magadiite, respectively.

Aside from the ability of the long alkyl ammonium intercalants to increase the clay interlayer spacing, they create a more favorable organophilic environment. The presence of the alkyl chains in the intergalleries of the organoclays lowers the surface energy of the host clay and improves the compatibility of the clay to become more miscible with the organic polymer matrix [38-39].

The amount of alkyl ammonium ions that can be intercalated between the clay layers is based on the charge exchange capacity (CEC) value of the clay being considered as a filler for a polymeric matrix. The candidate filler should have a CEC value between 0.5 – 2.0 meq/g of clay. Clays having less than 0.5 meg/g clay would lead to a small amount of organic intercalant after an ion exchange reaction. More than 2.0 meq/g of clay exchange capacity, the strength of the interlayer bonding is too high for easy intercalation [40]. Hence, montmorillonite clays having a CEC value of 0.93-1.2 meq/g of clay and vermiculites (CEC = 1.5 meq/g) [41] are ideal templates for intercalation.

The ion exchange reaction of these alkyl ammonium salts with the clay is reversible. Thus, in order to ensure a high conversion of a pristine MMT clay like in the case of sodium montmorillonite clay, Na^+-MMT, into an organoclay, an excess amount of the intercalating organic cation is usually observed:

$[NR_4]^+ + Na^+\text{-MMT} \quad [NR_4]^+\text{-MMT} + Na^+$

Lee and *Kim* (2003) [42] did a modification of Na^+-MMT clay using different amounts of an intercalating agent relative to the cation exchange capacity (CEC) of the clay. The intercalating agent used was a C_{16} ammonium salt, trimethylhexadecyl ammonium bromide, $CH_3(CH_2)_{14}CH_2N(CH_3)_2Br$. Different amounts of the intercalating agent were used, ranging from 0 to 3 times the CEC value of the Na^+-MMT. After the ion exchange reaction, the XRD profiles of the organoclays were obtained. The interlayer spacing of the produced organoclays was observed to increase with the amount of the alkyl intercalant. From the original value of d_{001}=1.4 nm (for Na^+-MMT), the interlayer distance increased to 1.9, 3.2 and 3.9 nm at a loading of 1, 2 and 3 times the CEC of the clay, respectively.

The alkyl ammonium intercalant can also provide functional groups which can react with the polymer matrix or supply sites for the initiation of a polymerization which can occur in the gaps between the clay platelets. This can be done by the introduction of an intercalating agent that possesses a functionality that can initiate the polymerization. After an ion exchange reaction with the highly exchangeable cations found in the galleries of the MMT layered structure, the tethered organic initiator can start the *in situ* polymerization where chains can be grown directly from the surface. The significance of an *in situ* polymerization after intercalation is based on the assumption that as the polymer chain grows, the silicate layers separate far apart until they become eventually exfoliated to form a well dispersed composite material [43]. *Zhou* et al. (2001) [44] explored this approach to prepare a clay-based polymer nanocomposite where polystyrene chains are directly grown from previously anchored initiators on the clay surfaces. First, the immobilization of a triethyl ammonium cation that contains 1,1-diphenylethylene (DPE) derivative through an ion exchange reaction with the sodium montmorillonite (Na^+-MMT) was performed. The DPE served as an initiator precursor. After the addition of n-butyl lithium (n-BuLi) and removal of the free n-BuLi from the reaction mixture, the polymerization of styrene was initiated directly from the ionically attached initiators on the clay surfaces.

3.2 Clay modification via silane-coupling reaction

One way of increasing the favorable interaction between organic molecules and clay surfaces is by introducing some hydrophobic groups onto the layer surfaces [45-46]. This method of clay modification can be possible with the reaction of silanes with the silanol groups found in the clay layered structure [10, 47-50]. The said technique makes use of the existing silanol groups found in the clay structure to react with organosilane agents. Silanol groups (Si-OH) are located on the clay edges due to broken edges and crystalline defects [51-56]. Using a chloro- or alkoxysilanes as a modifying agent, several functionalities can be introduced to the clay. Unlike the ion-exchanged clays, the covalently modified clays achieved through the hydrosilylation of the silanol groups are more thermally stable [47, 53]. More importantly, the characteristics of the modified clays can be easily fine tuned through the introduction of various end groups of the silane modifiers [52, 57].

Early studies on the use of silane agents in clay modification targeted the silanols found in the clay structure. In 1976, *Ruiz-Hitzky* et al. [58] used organochlorosilanes to hydrophobize the surfaces of sepiolite and chrysotile - both are examples of silicate materials. They were able to prepare different stable derivatives of the clays using organochlorosilanes. In modifying these layered silicate materials with the use of organosilanes to react with the silanol groups of the clay, they found out that only the external surfaces of the silicate clays can be modified as the grafting reaction can only access the edge silanols. Five years later [59], they reported the successful silylation of the internal silanols of a magadiite clay by suspending this clay in dimethylsulfoxide or N,N-dimethyl formamide. These solvents were able to expand the basal spacing of the layered silicic acid and permit the entry of the silane agent to reach the internal silanols of the H-magadiite. H-magadiite contains a lot of internal silanols which can be reacted with silane agents bearing various functionalities.

Park et al. (2004) [56] found that organic molecules intercalate much faster in the layered structure of laponite clay if the clay was first modified with octyltrimethoxysilane. The authors found that the grafting reaction of the silane agent only happens on the external surfaces of the laponite clay.

The covalent grafting of organosilanes through the reaction with silanols in the clay structure is important since it provides an opportunity to immobilize reactive organic groups to the clay via a stable covalent bond. Of primary interest, however, is to be able to chemically modify the interlayer surfaces of the silicate clay structure using this modification technique. Several authors have shown that this is possible. For example, in the case of *Ruiz-Hitzky* et al. (1985), after initially modifying the magadiite through the intercalation of polar organic molecules, the magadiite was successfully silylated by various organosilane reagents. The intercalation of polar organic agents increased the gaps between the layers. The grafting of organosilyl groups in the interlamellar space occurs due to

the larger gaps which make the interlamellar silanol (Si-OH) groups now more accessible to the silylating reagents [60].

The same success of grafting silane on the surface of kenyaite clay was achieved after performing gelification in the presence of octylamine and reaction at room temperature [61]. Kenyaite was also recently reacted with APTES and dodecylamine in ethanol, resulting in interlayer surface silylation. Magadiite and kenyaite are examples of natural minerals possessing a layered structure [62].

This modification route has been used in tandem with an ion exchange reaction to prepare nanocomposites [48, 63-65]. For example, in the work of *Yanagisawa* et al. (1988) [66] where they reported the successful silylation of the interlayer surface of layered polysilicic acids using a bulky group-bearing silane, diphenylmethylchlorosilane, utilizing these two methods. The layered acids, H-magadiite and H-kenyaite, were first modified with dodecyltrimethylammonium ion, $CH_3(CH_2)_{10}CH_2N^+(CH_3)_3$, to serve as the intermediates for the conversion. The intercalation of the ammonium salts enlarged the interlayer space allowing the bulky silylating agent to be intercalated. It was previously reported by *Ruiz-Hitzky* et al. (1985) [60] that a bulky silylating agent, like diphenylmethylchlorosilane, cannot be intercalated in these clays.

Some studies reported a combination of these methods to modify silicate clays. *Okutomo* et al. (1999) [49] for instance, reported the use of both alkyl ammonium modifier and silane agent to modify magadiite, a layered silicate clay. They used an ion exchange reaction technique to intercalate a dodecyltrimethylammonium cation, $CH_3(CH_2)_{10}CH_2N^+(CH_3)_3$, in order to increase the basal spacing of the clay. The larger gaps between platelets enabled the bulky chlorosilane to access the interlayer silanol groups of the magadiite clay. They also found out that by increasing the chain length of the silylating agent corresponded to an increase in the basal spacing of the silylated clay, the same effect observed when an alkyl ammonium salts are used as the intercalating agent. The advantage of the former is that the silane agent is attached to the clay by a more stable covalent attachment as opposed to an ionically-tethered ammonium alkyl chain.

He et al. (2005) [47] reported that the grafting reaction involving organosilanes reacting with layered silicates involves two steps. The silane molecules first intercalate into the clay interlayers followed by a condensation reaction between the silane molecules and the silanols of the clay layers.

Zhang et al. (2006) [48] were able to show that it is possible to successfully graft a silylating agent onto the internal surfaces of a silicate clay. This is important as this approach can provide an opportunity to anchor catalysts onto the silicate surfaces and facilitate polymerization inside the galleries. A commercial organoclay from Southern Clay Products, Inc,, Cloisite 20A, was used. An MMT clay derivative, modified with naturally-occurring tallow ammonium salt, was reacted with trimethylchlorosilane. The chlorosilane reacted with the edge hydroxyl groups of the clay, in the process, liberating HCl. The protons from the liberated HCl replaced some of the alkyl ammonium ions ionically attached between the clay platelets leading to the formation of new hydroxyl groups on the internal clay surfaces. Since an excess stoichiometric amount of the silylating agent was used, further silylation of the newly formed –OH groups was observed. The XRD profiles of the clay before and after silylation were compared. The product, TMS-20H, has a smaller basal spacing than the Cloisite 20A itself. This smaller gap confirmed the successful intercalation of the silylating agent since it has shorter length that the previously anchored tallow intercalant of Cloisite20A.

In another setup, the authors performed the same silylation process but in the presence of $NaHCO_3$. The authors reasoned out that if the protons from the liberated HCl during the silylation process were trapped by the hydrogen carbonate ions, only the edge silanol groups react with trimethylchlorosilane and there would be no change in the d_{001} spacing of the Cloisite20A due to the loss of the alkyl chain-bearing modifier. It was found that the silylation does not modify the internal MMT surfaces but only the edges in the presence of the bicarbonate ions as the resulting organoclay, labeled as TMS-20A, has the same basal spacing as the precursor. The results of the thermogravimetric analysis and infrared spectroscopy also confirmed the presence of the edge trimethylsilyl groups.

4. Conclusions

In the preparation of clay-based polymer nanocomposites, one particular challenge in using layered silicates like MMT as additives is getting the clay nanofillers to homogeneously mix with the matrix polymer. Modifying the clay filler before its incorporation in the polymer bulk is thus important. Two common clay modification methodologies are usually carried out: via ion-exchange reactions with alkyl cation salts and through silylation reactions. The most common method to modify clay fillers is to substitute the highly exchangeable cations originally found in the interlayers with long alkyl ammonium salts via ion exchange reactions. The intercalation of the alkyl chains in the galleries of the clay fillers leads to the expansion of the spaces between platelets. The intercalating agents also give more hydrophobic character to the modified clay fillers making them more compatible with organic polymers. Another method of clay modification is using organochlorosilanes. The use of silylation reactions to modify the surface of MMT clays is possible due to the presence of hydroxyl groups in the external and internal surfaces of MMT.

5. Acknowledgment

The author would like to thank Prof. Thomas AP Seery of the University of Connecticut for his insightful comments during the preparation of this article.

References

[1] Xie, W. – Gao, Z. – Pan, W-P. – Hunter, D. – Singh, A. – Vaia, R. (2001): Thermal degradation chemistry of alkyl quaternary ammonium montmorillonite. *Chemistry of Materials*. Vol. 13, No. 9, pp. 2979-90. https://doi.org/10.1021/cm010305s

[2] Alexandre, M. – Dubois, P. (2000): Polymer-layered silicate nanocomposites: preparation, properties and uses of a new class of materials. *Materials Science and Engineering: R: Reports*. Vol. 28. Nos. 1-2, pp. 1-63. https://doi.org/10.1016/S0927-796X(00)00012-7

[3] Tjong, S. C. – Meng, Y. Z. – Hay, A. S. (2001): Novel preparation and properties of polypropylene-vermiculite nanocomposites. *Chemistry of Materials*. Vol. 14, No. 1, pp. 44-51. https://doi.org/10.1021/cm010061b

[4] Kotek, J. – Kelnar, I. – Studenovský, M. – Baldrian, J. (2005): Chlorosulfonated polypropylene: preparation and its application as a coupling agent in polypropylene-clay nanocomposites. *Polymer*. Vol. 46, No. 13, pp. 4876-81. https://doi.org/10.1016/j.polymer.2005.02.119

[5] Pramoda, K. P. – Liu, T. (2004). Effect of moisture on the dynamic mechanical relaxation of polyamide-6/clay nanocomposites. *Journal of Polymer Science Part B: Polymer Physics*. Vol. 42, No. 10, pp. 1823-30. https://doi.org/10.1002/polb.20061

[6] Penaloza, D. P. – Sandberg, D. J. – Giotto, M. V. – Seery, T. A. P. (2015): An exfoliated clay-poly(norbornene) nanocomposite prepared by metal-mediated surface-initiated polymerization. *Polymer Engineering and Science*. Vol. 55, No. 10, pp. 2349-54. https://doi.org/10.1002/pen.24123

[7] Penaloza, D. P. (2016): Mechanical and thermal properties of clay-poly(norbornene) nanocomposites from ruthenium alkylidene-mediated surface-initiated polymerization. *Kimika*. Vol. 27, No. 1, pp. 23-9. https://doi.org/10.26534/kimika.v27i1.22-28

[8] Penaloza, D. P. (2017): Review on the preparation, structure and property relation of clay-based polymer nanocomposites. *Kimika*. Vol. 28. No. 1, pp. 44-56. https://doi.org/10.26534/kimika.v28i1.44-56

[9] Bee, S-L. – Abdullah, M. A. A. – Bee, S-T. – Sin, L. T. – Rahmat, A. R. (2018): Polymer nanocomposites based on silylated-montmorillonite: A review. *Progress in Polymer Science*. Vol.85, pp. 57-82. https://doi.org/10.1016/j.progpolymsci.2018.07.003

[10] Zhang, Z. H. – Li, T. S. – Yang, F. – Fu, C. G. (1998): Montmorillonite clay catalysis XI: Protection and deprotection of hydroxyl group by formation and cleavage of trimethylsilyl ethers catalysed by montmorillonite K-10. *Synthetic Communications*. Vol. 28, No. 16, pp. 3105-14. https://doi.org/10.1080/00397919808004891

[11] Tyan, H. L. – Liu, Y. C. – Wei, K. H. (1999): Thermally and mechanically enhanced clay/polyimide nanocomposite via reactive organoclay. *Chemistry of Materials*. Vol. 11, No. 7, pp. 1942-7. https://doi.org/10.1021/cm990187x

[12] Francis, V. – Jain, P. K. (2018): Surface enhancement approach for FDM rapid prototypes by organically modified montmorillonite nanoparticles. *IOP Conference Series: Materials Science and Engineering*.Vol. 383, No. 1, pp. 012010. https://doi.org/10.1088/1757-899X/383/1/012010

[13] Zare, Y. – Rhee, K. Y. (2017): Multistep modeling of Young's modulus in polymer/clay nanocomposites assuming the intercalation/exfoliation of clay layers and the interphase between polymer matrix and nanoparticles. *Composites Part A: Applied Science and Manufacturing*. Vol. 102, pp. 137-44. https://doi.org/10.1016/j.compositesa.2017.08.004

[14] Wang, W. – Zhao, Y. – Yi, H. – Chen, T. – Kang, S. – Li, H. – Song, S. (2018): Preparation and characterization of self-assembly hydrogels with exfoliated montmorillonite nanosheets and chitosan. *Nanotechnology*. Vol. 29, No. 2, pp. 025605. https://doi.org/10.1088/1361-6528/aa9ba4

[15] Dhatarwal, P. – Sengwa, R. J. – Choudhary, S. (2017): Effect of intercalated and exfoliated montmorillonite clay on the structural, dielectric and electrical properties of plasticized nanocomposite solid polymer electrolytes. *Composites Communications*. Vol. 5, pp.1-7. https://doi.org/10.1016/j.coco.2017.05.001

[16] Ji, J. – Ke, Y. – Pei, Y. – Zhang, G. (2017): Effects of highly exfoliated montmorillonite layers on the properties of clay reinforced terpolymer nanocomposite plugging microspheres. *Journal of Applied Polymer Science*. Vol. 134, No. 21, pp. 44894. https://doi.org/10.1002/app.44894

[17] Olphen, O. V. (1977): An introduction to clay colloid chemistry. *Journal of Pharmaceutical Sciences*. Vol 53, pp. 230-230. https://doi.org/10.1002/jps.2600530238

[18] Tjong, S. C. (2006): Structural and mechanical properties of polymer nanocomposites. *Materials Science and Engineering: R: Reports*. Vo. 53, Nos. 3-4, pp. 73-197. https://doi.org/10.1016/j.mser.2006.06.001

[19] Jeong, C. J. – Kang, E. B. – Park, S. J. – Choi, K. H. – Shin, G. – In, I. – Park, S. Y. (2015): Preparation of exfoliated montmorillonite nanocomposites with catechol/zwitterionic quaternized polymer for an antifouling coating. *Polymer Engineering & Science*. Vol. 55, No. 9, pp. 2111-7. https://doi.org/10.1002/pen.24052

[20] Horst, M. F. – Quinzani, L. M. – Failla, M. D. (2014): Rheological and barrier properties of nanocomposites of HDPE and exfoliated montmorillonite. *Journal of Thermoplastic Composite Materials*. Vol. 27, No. 1, pp. 106-25. https://doi.org/10.1177/0892705712443248

[21] Follain, N. – Alexandre, B. – Chappey, C. – Colasse, L. – Médéric, P. – Marais, S. (2016): Barrier properties of polyamide 12/montmorillonite nanocomposites: Effect of clay structure and mixing conditions. *Composites Science and Technology*. Vol. 136, pp. 18-28. https://doi.org/10.1016/j.compscitech.2016.09.023

[22] Endo, K. – Sugahara, Y. – Kuroda, K. (1994): Formation of intercalation compounds of a layered sodium octosilicate with N-alkyltrimethylammonium ions and the application to organic derivatization. *Bulletin of the Chemical Society of Japan*. Vol. 67, No. 12, pp. 3352-5. https://doi.org/10.1246/bcsj.67.3352

[23] Ogawa, M. – Kuroda, K. (1997): Preparation of inorganic-organic nanocomposites through intercalation of organoammonium ions into layered silicates. *Bulletin of the Chemical Society of Japan*. Vol. 70, No. 11, pp. 2593-618. https://doi.org/10.1246/bcsj.70.2593

[24] Fudala, A. – Palinko, I. – Kiricsi, I. (1999): Preparation and characterization of hybrid organic-inorganic composite materials using the amphoteric property of amino acids: Amino acid intercalated layered double hydroxide and montmorillonite. *Inorganic Chemistry*. Vol. 38, No. 21, pp. 4653-8. https://doi.org/10.1021/ic981176t

[25] Matsumoto, A. – Odani, T. – Sada, K. – Miyata, M. – Tashiro, K. (2000): Intercalation of alkylamines into an organic polymer crystal. *Nature*. Vol. 405, No. 6784, pp. 328-30. https://doi.org/10.1038/35012550

[26] Pálková, H. – Zimowska, M. – Jankovič, Ľ. – Sulikowski, B. – Serwicka, E. M. – Madejová, J. (2017): Thermal stability of tetrabutyl-phosphonium and -ammonium exchanged montmorillonite: Influence of acid treatment. *Applied Clay Science*. Vol. 138, pp. 63-73. https://doi.org/10.1016/j.clay.2016.12.043

[27] Osman, M. A. – Ploetze, M. – Skrabal, P. (2004): Structure and properties of alkylammonium monolayers self-assembled on montmorillonite platelets. *The Journal of Physical Chemistry B*. Vol. 108, No. 8, pp. 2580-8. https://doi.org/10.1021/jp0366769

[28] Fornes, T. D. – Yoon, P. J. – Hunter, D. L. – Keskkula, H. – Paul, D. R. (2002): Effect of organoclay structure on nylon 6 nanocomposite morphology and properties. *Polymer*. Vol. 43, No. 22, pp. 5915-33. https://doi.org/10.1016/S0032-3861(02)00400-7

[29] Huskic, M. – Zagar, E. – Zigon, M. – Brnardic, I. – Macan, J. – Ivankovic, M. (2009): Modification of montmorillonite by cationic polyesters. *Applied Clay Science*. Vol. 43, No. 3-4, pp. 420-4. https://doi.org/10.1016/j.clay.2009.01.008

[30] Xie, W. – Gao, Z. – Liu, K. – Pan, W-P. – Vaia, R. – Hunter, D. – Singh, A. (2001): Thermal characterization of organically modified montmorillonite. *Thermochimica Acta*. Vol. 367-368, pp. 339-50. https://doi.org/10.1016/S0040-6031(00)00690-0

[31] Kooli, F. (2009): Thermal stability investigation of organo-acid-activated clays by TG-MS and in situ XRD techniques. *Thermochimica Acta*. Vol. 486, Nos. 1-2, pp. 71-6. https://doi.org/10.1016/j.tca.2008.12.025

[32] Lagaly, G. (1986): Interaction of alkylamines with different type of layered compounds. *Solid State Ionics*. Vol. 22, pp. 43-51. http://dx.doi.org/10.1016/0167-2738(86)90057-3

[33] Fu, Y-T. – Heinz, H. (2010): Structure and cleavage energy of surfactant-modified clay minerals: Influence of CEC, head group and chain length. *Philosophical Magazine*. Vol. 90, No. 17, pp. 2415-24. https://doi.org/10.1080/14786430903559490

[34] Kloprogge, J. T. (1998): Synthesis of smectites and porous pillared clay catalysts: a review. *Journal of Porous Materials*. Vol. 5, No. 1, pp. 5-41. https://doi.org/10.1023/A:1009625913781

[35] Osman, M. A. – Ernst, M. – Meier, B. H. – Suter, U. W. (2001): Structure and molecular dynamics of alkane monolayers self-assembled on mica platelets. *The Journal of Physical Chemistry B*. Vol. 106, No. 3, pp. 653-62. https://doi.org/10.1021/jp0132376

[36] Vaia, R. A. – Teukolsky, R. K. – Giannelis, E. P. (1994): Interlayer structure and molecular environment of alkylammonium layered silicates. *Chemistry of Materials*. Vol. 6, No. 7, pp. 1017-22. https://doi.org/10.1021/cm00043a025

[37] Hackett, E. – Manias, E. (1998): Molecular dynamics simulations of organically modified layer silicates. *Journal of Chemical Physics*. 1998;108(17):7410. https://doi.org/10.1063/1.476161

[38] Blumstein, A. (1965): Polymerization of adsorbed monolayers. II. Thermal degradation of the inserted polymer. *Journal of Polymer Science Part A: General Papers*. Vol. 3, No. 7, pp. 2665-72. https://doi.org/10.1002/pol.1965.100030721

[39] Krishnamoorti, R. – Vaia, R. A. – Giannelis, E. P. (1996): Structure and dynamics of polymer-layered silicate nanocomposites. *Chemistry of Materials*. Vol. 8, No. 8, pp. 1728-34. https://doi.org/10.1021/cm960127g

[40] Utracki, L. A. – Sepehr, M. – Boccaleri, E. (2007): Synthetic, layered nanoparticles for polymeric nanocomposites (PNCs). *Polymers for Advanced Technologies*. Vol. 18, No. 1, pp. 1-37. https://doi.org/10.1002/pat.852

[41] Ray, S. S. – Okamoto, K. – Okamoto, M. (2003): Structure-property relationship in biodegradable poly(butylene succinate)/layered silicate nanocomposites. *Macromolecules*. Vol. 36, No. 7, pp. 2355-67. https://doi.org/10.1021/ma021728y

[42] Lee, S. Y. – Kim, S. J. (2003): Dehydration behavior of hexadecyltrimethylammonium-exchanged smectite. *Clay Minerals*. Vol. 38, No. 2, pp. 225-32. https://doi.org/10.1180/0009855033820091

[43] Fan, X. – Zhou, Q. – Xia, C. – Cristofoli, W. – Mays, J. – Advincula, R. (2002): Living anionic surface-initiated polymerization (LASIP) of styrene from clay nanoparticles using surface bound 1,1-diphenylethylene (DPE) initiators. *Langmuir*. Vol. 18, No. 11, pp. 4511-8. https://doi.org/10.1021/la025556+

[44] Zhou, Q. – Fan, X. – Xia, C. – Mays, J. – Advincula, R. (2001): Living anionic surface initiated polymerization (SIP) of styrene from clay surfaces. *Chemistry of Materials*. Vol. 13, No. 8, pp. 2465-7. https://doi.org/10.1021/cm0101780

[45] Herrera, N. N. – Letoffe, J. M. – Putaux, J. L. – David, L. – Bourgeat-Lami, E. (2004): Aqueous dispersions of silane-functionalized laponite clay platelets. A first step toward the elaboration of water-based polymer/clay nanocomposites. *Langmuir*. Vol. 20, No. 5, pp. 1564-71. https://doi.org/10.1021/la0349267

[46] Romanzini, D. – Frache, A. – Zattera, A. J. – Amico, S. C. (2015): Effect of clay silylation on curing and mechanical and thermal properties of unsaturated polyester/montmorillonite nanocomposites. *Journal of Physics and Chemistry of Solids*. Vol. 87, pp. 9-15. https://doi.org/10.1016/j.jpcs.2015.07.019

[47] He, H. P. – Duchet, J. – Galy, J. – Gerard, J. F. (2005): Grafting of swelling clay materials with 3-aminopropyltriethoxysilane. *Journal of Colloid and Interface Science*. Vol. 288, No.1, pp. 171-6. https://doi.org/10.1016/j.jcis.2005.02.092

[48] Zhang, J. G. – Gupta, R. K. – Wilkie, C. A. (2006): Controlled silylation of montmorillonite and its polyethylene nanocomposites. *Polymer*. Vol. 47, No. 13, pp. 4537-43. https://doi.org/10.1016/j.polymer.2006.04.057

[49] Okutomo, S. – Kuroda, K. – Ogawa, M. (1999): Preparation and characterization of silylated-magadiites. *Applied Clay Science*. Vol. 15, No. 1-2, pp. 253-64. https://doi.org/10.1016/S0169-1317(99)00010-1

[50] Ogawa, M. – Okutomo, S. – Kuroda, K. (1998): Control of interlayer microstructures of a layered silicate by surface modification with organochlorosilanes. *Journal of the American Chemical Society*. Vol. 120, No. 29, pp. 7361-2. https://doi.org/10.1021/ja981055s

[51] Deuel, H. – Huber, G. – Iberg, R. (1950): Organische derivate von tonmineralien. *Helvetica Chimica Acta*. Vol. 33, No. 5, pp. 1229-32. https://doi.org/10.1002/hlca.19500330514

[52] Letoffe, J-M. – Putaux, J-L. – David, L. – Bourgeat-Lami, E. (2004): Aqueous dispersions of silane-functionalized laponite clay platelets. A first step toward the elaboration of water-based polymer/clay nanocomposites. *Langmuir*. Vol. 20, No. 5, pp. 1564-71. https://doi.org/10.1021/la0349267

[53] Song, K. – Sandi, G. (2001): Characterization of montmorillonite surfaces after modification by organosilane. *Clays and Clay Minerals*. Vol. 49, No. 2, pp. 119-25.

[54] Herrera, N. N. – Letoffe, J-M. – Reymond, J-P. – Bourgeat-Lami, E. (2005): Silylation of laponite clay particles with monofunctional and trifunctional vinyl alkoxysilanes. *Journal of Materials Chemistry*. Vol. 15, No. 8, pp. 863-71. https://doi.org/10.1039/B415618H

[55] Lee, D. C. – Jang, L. W. (1996): Preparation and characterization of PMMA-Clay hybrid composite by emulsion polymerization. *Journal of Applied Polymer Science*. Vol. 61, No. 7, pp. 1117-22. https://doi.org/10.1002/(SICI)1097-4628(19960815)61:7<1117::AID-APP7>3.0.CO;2-P

[56] Park, M. – Shim, I-K. – Jung, E-Y. – Choy, J-H. (2004): Modification of external surface of laponite by silane grafting. *Journal of Physics and Chemistry of Solids*. Vol. 65, Nos. 2-3, pp. 499-501. https://doi.org/10.1016/j.jpcs.2003.10.031

[57] Wheeler, P. A. – Wang, J. – Baker, J. – Mathias, L. J. (2005): Synthesis and characterization of covalently functionalized laponite clay. *Chemistry of Materials*. Vol. 17, No. 11, pp. 3012-8. https://doi.org/10.1021/cm050306a

[58] Ruiz-Hitzky, E. – Fripiat, J. J. (1976): Organomineral derivatives obtained by reacting organochlorosilanes with the surface of silicates in organic solvents. *Clays and Clay Minerals*. Vol. 24, No. 1, pp. 25-30. https://doi.org/10.1346/CCMN.1976.0240102

[59] Ruiz-Hitzky, E. R. – Rojo, J. M. (1980): Intracrystalline grafting on layer silicic acids. *Nature*. Vol. 287, pp. 28-30. https://doi.org/10.1038/287028a0

[60] Ruiz-Hitzky, E. R. – Rojo, J. M. – Lagaly G. (1985): Mechanism of the grafting of organosilanes on mineral surfaces. *Colloid & Polymer Science*. Vol. 263, No. 12, pp. 1025-30. https://doi.org/10.1007/BF01410996

[61] Thiesen, P. H. – Beneke, K. – Lagaly, G. (2002): Silylation of a crystalline silicic acid: an MAS NMR and porosity study. *Journal of Materials Chemistry*. Vol. 12, No. 10, pp. 3010-5. https://doi.org/10.1039/B204314A

[62] Eugster, H. P. (1967): Hydrous sodium silicates from Lake Magadi, Kenya: precursors of bedded chert. *Science*. Vol. 157, No. 3793, pp. 1177-80. https://doi.org/10.1126/science.157.3793.1177

[63] Chen, G-X. – Choi, J. B. – Yoon, J. S. (2005): The role of functional group on the exfoliation of clay in poly(L-lactide). *Macromolecular Rapid Communications*. Vol. 26, No. 3, pp. 183-7. https://doi.org/10.1002/marc.200400452

[64] Chen, G-X – Kim, H-S – Shim, J-H – Yoon, J-S. (2005): Role of epoxy groups on clay surface in the improvement of morphology of poly(l-lactide)/clay composites. *Macromolecules*. Vol. 38, No. 9, pp. 3738-44. https://doi.org/10.1021/ma0488515

[65] Wheeler, P. A. – Wang, J. – Mathias, L. J. (2006): Poly(methyl methacrylate)/laponite nanocomposites: exploring covalent and ionic clay modifications. *Chemistry of Materials*. Vol. 18, No. 17, pp. 3937-45. https://doi.org/10.1021/cm0526361

[66] Yanagisawa, T. – Kuroda, K. – Kato, C. (1988): Organic derivatives of layered polysilicates. II. Reaction of magadiite and kenyaite with diphenylmethylchlorosilane. *Bulletin of the Chemical Society Japan*. Vol. 61, No. 10, pp. 3743-3745. https://doi.org/10.1246/bcsj.61.3743

Ref.:
Penaloza, David P. Jr.: *Modified clay for the synthesis of clay-based nanocomposites*
Építőanyag – Journal of Silicate Based and Composite Materials, Vol. 71, No. 1 (2019), 5–11. p.
https://doi.org/10.14382/epitoanyag-jsbcm.2019.2

Mathematical modelling: case of Haoud Berkaoui

Abderrahmane MELLAK ▪ Hydrocarbons and Chemicals Faculty – Director of Laboratory of Hydrocarbon Engineering (LGPH), Université M'Hamed Bougara de Boumerdès, Algérie.

Érkezett: 2018. 08. 18. ▪ Received: 18. 08. 2018. ▪ https://doi.org/10.14382/epitoanyag-jsbcm.2019.3

Abstract

Research has been done in the Physics Laboratory in the School and Observatory Physics of Strasbourg consist of placing in a theoretical frame necessary to a better comprehension of the severe problem of the collapsing of the Haoud Berkaoui well (creation of a huge underground cave and important collapsing of the surface ground due to a bad drilling of a petroleum well in the south of Algeria) and especially mathematical modelling.

Keywords: geomechanics, Haoud Berkaoui, environment, major collapsing, rupture criterion, modelling.

Kulcsszavak: geomechanika, Haoud Berkaoui, környezet, kiterjedt tönkremenetel, törési feltétel, modellezés.

Prof. Abderrahmane MELLAK

Director of the Laboratory of Engineering Physics of Hydrocarbons and Professor and Researcher Lecturer at the Faculty of Hydrocarbons and Chemistry of the University of Boumerdes, Algeria. He is an engineer in Oil Drilling (graduated in Algeria) and also holds a DEA (Diploma of Advanced Studies), a DESS (Diploma of Specialized Higher Studies) and a PhD, obtained in French Universities. Responsible for a team of researchers, Head of Bachelor and Master Drilling Wells, frames of United Engineers, Master, the Magister and Doctorates. Member of the National Commission of University Habilitation Programs (CNH) and the National Commission for the Evaluation of Algerian Universities (CNE), the Ministry of Higher Education and Scientific Research. Participated in world congresses and national and international conferences with papers and has several publications in recognized national and international journals. Participated in several television round tables (Canal Algeria, UFC) on the Quality of Higher Education, the University-Business Relationship). Attended the 26th World Gas Congress (WGC), held in Paris from June 1st to 5th, 2015.

1. Introduction

The problem of Haoud Berkaoui is a difficult problem to solve, it is a rare case and perhaps unique in the world. The research work developed mainly at the School and Observatory of Physics of the Globe of Strasbourg (Mellak, A., Reuschlé, T. and Gueguen Y, 1990) essentially consists in the modelling of the delicate problem of collapse of the oil well of Haoud Berkaoui. An oil well was drilled, which never reached its objective because of many technical problems including the uncontrolled eruption of the Albian; very large freshwater aquifer zone (this water table is about 500 m thick and extends over several hundred kilometers) and very eruptive (it is located at about 1000 m deep and has a pressure of 13.8 MPa), that created a large hole underground by leaching out of the salt formation.

Fig. 1. Satellite photo of 14 January 2015 showing Haoud Berkaoui crater with a diameter of approximately 350 m (Credits: Google Earth)

1. ábra A Haoud Berkaoui kráter műholdképe 2015. január 14-én; a kráter átmérője kb. 350 m

In fact, the Albian's freshwater is pressurized back to the salt (this layer is about 200 m thick), the sodium chloride dissolves, and the salty water has taken the place of the salt. This dissolution of the sodium chloride enlarged the subterranean hole, and after a while, large surface cracks formed, followed by a major collapse creating an imposing crater of about 350 m in diameter and about a hundred meters deep (*Fig. 1*). While currently the surface dimensions of the big hole of Berkaoui are known, the boundaries of the underground hole are imprecise.

The present research work consists of:

1. Modelling of the underground hole into an elliptically shaped hole (this is the geometric form that can be closer to the real case and can be treated by simple methods);
2. Determination of the complex potentials according to the geometries encountered (case of the ellipse);
3. Calculation of stress and displacement fields at the surface;
4. Programming (in Fortran) of the problem considering two cases:
   a) Cases where the pressure is considered uniform in the underground cavity,
   b) Cases where the pressure is not uniform in the underground cavity.
5. Plots and interpretation of the curves of stresses and displacements;
6. Determination of a criterion of rupture.

2. Modelling

The problem of Haoud Berkaoui (HBK) can be treated as a first approximation as a plane elasticity problem in an infinite medium. We consider a system consisting of an infinite thin plate pierced with a hole (the underground cavity) approximated in this case by an ellipse. The center of this ellipse is located at a distance H from a line representing the plot of the Earth's surface (H represents the depth of the center of the ellipse). The long axis of the ellipse is parallel with the straight line (the cavity is horizontal) and it is considered that the fluid pressure inside the cavity is negligible compared to the weight of the overlying terrain.

In fact, we try in our case to do a modeling of the elastic deformation in the plate especially at the level of the line on the surface. Surface deformations are significant in the case of HBK (collapses, wide and deep fissures). Also, in order to examine the mechanical relation between the hole loading and the rupture process, we neglect at first the geometrical irregularities (the surface of the Earth is not uniformly flat) and the non-homogeneity of the terrains by compared to the elastic modulus.

In order to make the problem mathematically treatable we assume that the plate is homogeneous and isotropic. Let *a* and *b* be the half-big and small axes of the ellipse respectively. The major axis of the ellipse is carried by the abscissa axis (Ox). It is a question of calculating the complex potentials *(z), where z = x + iy, knowing the conditions of constraints to the limits imposed on the system.

3. Transformation of the plane

To solve the problem, we proceed to a change of variable which makes the point M(z) of the plane (O, x, y) the image by the conformal transformation ω of a point P(ζ) of the plane (O, ζ_1, ζ_2) with :

$$z = \omega(\zeta) = R(\zeta + m\,\zeta^{-1}) \qquad R > 0,\ m \geq 0 \tag{1}$$

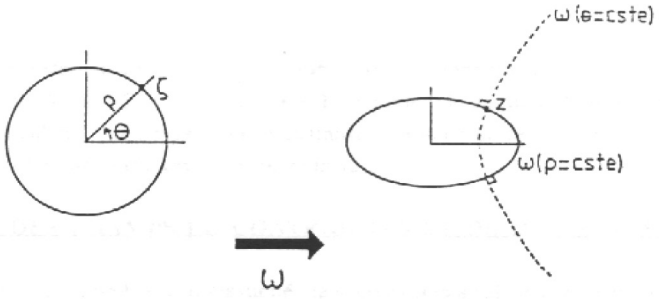

Fig. 2. Transformation of the plane
2. ábra Síktranszformáció

A circle of radius ρ is transformed into an ellipse ω(ρ = constant), and the direction line θ into a branch of hyperbola ω(θ = constant). The two curves are orthogonal in $z = \omega(\zeta)$.

We see $\zeta = \rho\, e^{i\theta}$, that this transformation corresponds to a circle (ρ = constant) of the plane (O, ζ_1, ζ_2) an ellipse in the plane (O, x, y) (*Fig. 2.*). The half-axes of the ellipse are given by:

$$a = R(\rho + m.\ \rho^{-1}) \qquad b = R(\rho\ - m.\ \rho^{-1})$$

By putting R = (a + b) / 2 and m = (a – b) / (a + b), we find that the elliptic hole is the image of the circle of radius $\rho = 1$ in the plane (O, ζ_1, ζ_2), that is to say that at every point of the ellipse is associated a point ζ such that $|\zeta| = 1$. *Fig. 3* illustrates the relation between θ and the position of M(z) on the ellipse.

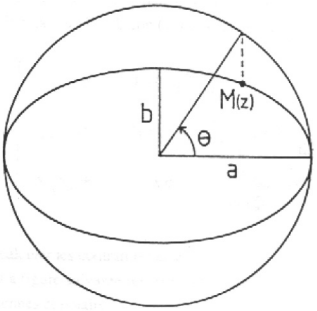

Fig. 3. Relationship between θ and the position of M(z) on the ellipse
3. ábra Kapcsolat a θ szög és az M(z) függvény között az ellipszisen

The domain outside the ellipse, ie the solid, corresponds in the plane (O, ζ_1, ζ_2) to the domain in which $|\zeta| \geq 1$. When m = 1, we obtain the case of the crack and for m = 0 the case of the circular hole. So from this transformation of a circle, we will be able to solve the different cases in our work.

4. Calculation of the fields of constraints and displacement

The resolution of a plane elasticity problem will consist of calculating the complex potentials $\varphi(z)$ and $\psi(z)$, and then calculating the stress and displacement fields at any point M(x, y) of the solid using the relations of Kolosov-Muskhelishvili (Muskhelishvili, 1977) which define the plane state from potentials φ and ψ.

$$\begin{cases} \sigma_{xx} + \sigma_{yy} = 4\,\Re e\left[\varphi'(z)\right] \\ \sigma_{yy} - \sigma_{xx} + 2i\sigma_{xy} = 2\left[\overline{z}\,\varphi''(z) + \psi'(z)\right] \\ 2M\left(u_x + iu_y\right) = \kappa\varphi(z) - z\,\varphi'(z) - \overline{\psi(z)} \end{cases} \tag{2}$$

with:
M = *E* / 2(1+ νν) = shear modulus of the solid;
κκ = 3 - 4 νν (case of plane deformation);
νν = Poisson's ratio;
E = Young's modulus.

σs_{xx}, σs_{yy} and σs_{xy} are the normal and tangential constraints, U_x and U_y are the horizontal and vertical displacements. By referring the relation (1) in equations (2) we obtain:

$$\begin{cases} \sigma_{xx} + \sigma_{yy} = 4\,\Re e\left[\dfrac{\varphi'(\zeta)}{\omega'(\zeta)}\right] \\ \sigma_{yy} - \sigma_{xx} + 2i\sigma_{xy} = \dfrac{2}{\omega'(\zeta)}\left[\overline{\omega(\zeta)}\ \dfrac{d}{d\zeta}\left(\dfrac{\varphi'(\zeta)}{\omega'(\zeta)}\right) + \psi'(\zeta)\right] \\ 2M\left(u_x + iu_y\right) = \kappa\varphi(\zeta) - \dfrac{\omega(\zeta)}{\omega'(\zeta)}\ \overline{\varphi'(\zeta)} - \overline{\psi(\zeta)} \end{cases} \tag{3}$$

It is also possible to calculate the stresses and displacements in polar coordinates (ρ, θ) in the plane (O, x, y). *Fig. 4* shows components of the stress tensor in Cartesian and polar coordinates.

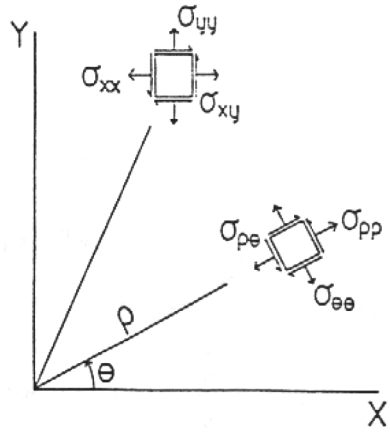

Fig. 4. Representation of the components of the stress stretcher in Cartesian and Polar coordinates
4. ábra Feszültségkomponensek reprezentációja derékszögű és poláris koordinátarendszerekben

For the computation of the stresses and displacements in polar coordinates one uses the laws of transformations following (Muskhelishvili, 1977):

$$\begin{cases} \sigma_{\rho\rho} + \sigma_{\theta\theta} = \sigma_{xx} + \sigma_{yy} \\ \sigma_{\theta\theta} - \sigma_{\rho\rho} + 2i\sigma_{\rho\theta} = e^{2i\alpha}\left(\sigma_{yy} - \sigma_{xx} + 2i\sigma_{xy}\right) \\ u_\rho + iu_\theta = e^{-i\alpha}\left(u_x + iu_y\right) \end{cases} \quad (4)$$

α is defined as follows. Let P(ζ) be a point on the plane plan (O, ζ1, ζ2) and ω*P)(z*, its image in the plane (O, x, y). By the transformation ωω, the line Δ(θ = constant) is transformed into the hyperbola branch ω(Δ). α is the angle the tangent makes to ω(Δ) in ω(P) white (Ox).

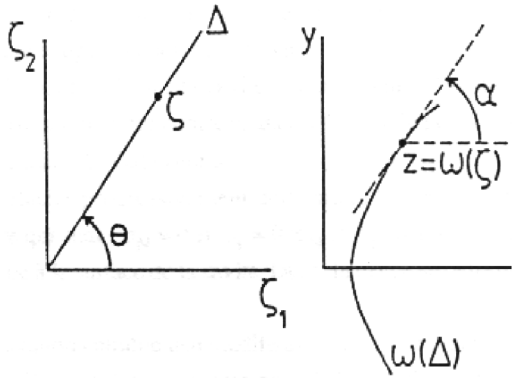

Fig. 5. Transformation of line Δ(θ = constant) into hyperbolic branch ω(Δ)
5. ábra Vonaltranszformáció Δ(θ = konstans) hiperbolává ω(Δ)

In other words, α is the angle, in z = ω(ζ), between the normal to the ellipse image of the circle (ρ = constant) and (Ox). We show that:

$$e^{i\alpha} = \frac{\varsigma^2}{\rho^2}\frac{\omega'(\varsigma)}{\omega'(\varsigma)}$$

By referring (4) to (3), we obtain:

$$\begin{cases} \sigma_{\rho\rho} + \sigma_{\theta\theta} = 4\,\Re e\left[\dfrac{\varphi'(\zeta)}{\omega'(\zeta)}\right] \\ \sigma_{\theta\theta} - \sigma_{\rho\rho} + 2i\sigma_{\rho\theta} = \dfrac{2\zeta^2}{\rho^2}\dfrac{1}{\omega'(\zeta)}\left[\overline{\omega(\zeta)}\,\dfrac{d}{d\zeta}\left(\dfrac{\varphi'(\zeta)}{\omega'(\zeta)}\right) + \psi'(\zeta)\right] \\ 2M\left(u_\rho + iu_\theta\right) = \dfrac{\overline{\zeta}}{\rho}\dfrac{\overline{\omega'(\zeta)}}{\left|\omega'(\zeta)\right|}\left[\kappa\varphi(\zeta) - \dfrac{\omega(\zeta)}{\omega'(\zeta)}\,\overline{\varphi'(\zeta)} - \overline{\psi(\zeta)}\right] \end{cases} \quad (5)$$

Relationships (5) are useful when one is interested in the state of stresses at the surface of the elliptic hole (ρρ =1) since $\sigma_{\rho\rho}$, $\sigma_{\theta\theta}$ and $\sigma_{\rho\theta}$ are the normal and tangential stresses at the surface. We will therefore calculate the potentials φφ and ψψ according to the variable ζζ and then using the transformation z = ωω(ζζ), we will be able to calculate the stresses and displacements in the plane (O, x, y).

5. Computer programming

To study the problem of Haoud Berkaoui, we followed the procedure:

- Before the dissolution of the sodium chloride by the water of the Albian, there is continuity of the stresses through the surface of the potential cavity. The stress along this surface is vertical and equal to the weight of the overlying land.
- Subsequently the salt is dissolved in the cavity but fictitiously maintained inside the cavity a stress field which counterbalances the weight of the ground in every point of the surface: the system remains in its original state.
- This constraint is gradually released to reach the new equilibrium conditions which are: $\sigma_N = 0$ and $\sigma_T = 0$ (free surface) where σ_N and σ_T are the normal and tangential stresses to the cavity surface. During this relaxation, the cavity is deformed elastically.

Relaxation causes a modification of the displacement and stress fields inside the surrounding environment, especially on the surface of the Earth. To calculate these different fields, we consider that the new equilibrium situation corresponds to the conditions that prevail in the medium for a cavity charged by σ_{0N} and σ_{0T}, the normal and tangential stresses applied to the surface of the cavity before relaxation, that is to say related to the weight of the grounds.

The weight of the grounds or lithostatic stress is given by:

$$\sigma_V = dgh$$

with:
d = density of the land;
g = acceleration of gravity;
h = depth

This stress varies along the surface of the cavity as a function of the depth of the point of application. This point $z = x + iy$ is the image of a point $\zeta = \rho\, e^{i\theta}$ by the transformation ω. The depth *h* of this point and its y-coordinate in a coordinate system linked to the center of the cavity are linked by $h = H - y$. Now, y = b sin (*). And the constraint V is thus given by: V is thus given by: σ by the transformation (*). The depth h of this point

and its y-coordinate in a coordinate system linked to the center of the cavity are linked by h = H - y. Now, y = b sin θ . And the constraint σ_V is thus given by:

$$\sigma_V = dg\,(H - b \sin\theta)$$

Using relations (4), it is then possible to calculate at any point on the surface of the cavity the normal stress σ_{0V} (=$\sigma_{\rho\rho}$, $\sigma_{\theta\theta}$), and the tangential stress σ_{0V} = ($\sigma_{\rho\theta}$) associated.

The computer program will consist of the following sequence:

- Regular distribution of measurement stations of stress fields and displacements on the surface of the Earth;
- Cutting the contour of the cavity into a number of segments (generally 100). On each segment are calculated σ_{0T} and σ_{0N} depending on the depth of the mid-segment point;
- Calculating at each station the surface of the stresses and displacements due to σ_{0T} and σ_{0N} by using the complex potentials corresponding to this type of loading of an elliptical cavity segment;
- Summation of the effects of all the segments of the cavity of each station of the surface;
- Drawing of the stress curves and surface displacements by a suitable software.

Two cases can be distinguished according to whether or not the length of the minor axis of the cavity is neglected in front of its depth. In the first case, we can consider that we are in first approximation in the case of the cavity uniformly loaded by a normal stress $\sigma_{0N} = dg\,(H\text{-}b)$.

It is then not necessary to segment the contour of the cavity and one can use the simplified complex potentials corresponding to this loading geometry. In the second case, the procedure described above applies.

6. Trace and interpretation of curves

The parameters of the model that we retain are the following:

- half-major axis of the cavity a = 200 m;
- half-small axis b = 100 m;
- depth of the center of the cavity H = 448 m;
- average Young's modulus for the overlying layers E = 8-10-10 Pa;
- average Poisson's ratio v = 0.28;
- average density d = 2650 kg/m^3.

Except for a, the parameters were selected based on existing data and assuming that the entire thickness of the salt layer was dissolved. The value of *a* was chosen arbitrarily since no constraint allows to constrain it. The number of stations on the surface is n_s = 100 and the number of segments on the perimeter of the cavity is n_e = 100. Two series of curves have been drawn:

a) Case where the cavity is uniformly loaded: curves 1.1, 1.2, 1.3, 1.4 and 1.5.

b) Case where the cavity is not uniformly loaded: 2.1, 2.2, 2.3, 2.4 and 2.5.

For each case we have plotted the following curves:

Normal and tangential stresses at the surface:

1) σ_{xx}, = *f((x/a)*.
2) σ_{yy} = *f((x/a)*.
3) σ_{xy} = *f((x/a)*.

Vertical and horizontal surface displacements:

1) u_y = *f((x/a)*.
2) u_x = *f((x/a)*.

Table 1 shows the variations of the stress and displacement values plumb with the cavity (x = 0) for different values of a and b.

Dimensions			Constraints (10^5 Pa)			Displacement (10^{-3} m)	
a (m)	*b*(m)	H/a	σ_{xx}	σ_{yy}	σ_{xy}	u_x	U_y
100	50	4.48	23	1.32	34.40	5.40	3.19
200	100	2.24	47	1.54	79.40	7.90	4.11
300	150	1.49	72	1.87	122.10	8.69	5.79
400	200	1.12	97	9.90	156.00	20.80	17.40

Table 1 Variations of the calculated stress and displacement
1. táblázat Számított feszültségek és alakváltozások

7. Interpretation

The most interesting information that can be drawn from the curves and *Table 1* are:

a) In the case of Haoud Berkaoui (horizontal underground cavern approximated by an ellipse), we observe a maximum displacement perpendicular to the cavity and a symmetrical plot on both sides of this point, for the uniform loading. In non-uniform loading, the maximum is displaced laterally but the curve remains symmetrical. For the horizontal displacement, the curve passes by 0 in line with the hole and is antisymmetric with respect to this point. This observation is quite logical given the symmetry of loading.

b) Curves tend to zero to infinity: the effect of the cavity decreases with distance.

c) The normal stress σ_{yy} passes through a maximum above the hole for both types of loading and is symmetrical with respect to this point. It is the same for the horizontal stress σ_{xx} whereas the tangential stress σ_{xy} is antisymmetric and goes through zero at this point.

d) Surface displacements decrease when the depth / half-length ratio increases.

8. Determination of a rupture criterion

It is possible to determine graphically from which value of stress it is possible to have potential breaks in the surface. The three basic modes of rupture are represented by *Fig. 6*.

In the case of an extension rupture (vertical cracking), a criterion of the type $\sigma_{xx} \geq \sigma_0$, where σ_0 is the tensile strength of the rock. In the case of shear failure, a Mohr-Coulomb failure criterion is used:

$$|\sigma_T| \geq S_0 + \mu\,|\sigma_N|$$

with: σ_T = tangential stress applied along a potential plane of rupture;

σs_N = normal stress applied on the same plane;

S_0 = shear strength of the rock;

μ = coefficient of friction of the rock.

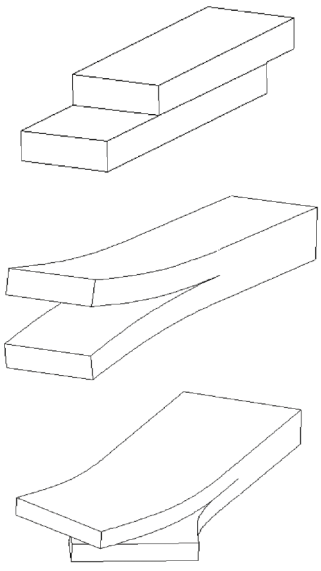

Mode I or Traction:
Perpendicular opening of the lips of the crack under the action constraints of extension.

Mode II or Shear:
Slip of the crack lips in a direction perpendicular to the front of the crack.

Mode III or Twist:
Relative sliding of the lips of the crack in a direction parallel to the front of the crack.

Fig. 6. Representation of the fundamental modes of rupture
6. ábra Jellegzetes törési módok bemutatása

In this case, look for the potential break plane (inclined to the horizontal). Thus, knowing σ_{xx}, σ_{xy} and σ_{yy} on the surface, we can calculate for a plane of inclination the values of σ_N and σ_T namely :

$$\sigma_N = \frac{\sigma_{xx} + \sigma_{yy}}{2} - \frac{\sigma_{xx} - \sigma_{yy}}{2} \cos 2\beta - \sigma_{xy} \sin 2\beta$$

$$\sigma_T = -\frac{\sigma_{xx} - \sigma_{yy}}{2} \sin 2\beta + \sigma_{xy} \cos 2\beta$$

The plane of rupture is that by which the preceding criterion is respected. To go beyond this qualitative analysis, real, accurate and up-to-date data is absolutely necessary.

9. Conclusions

The setting up of a theoretical framework necessary for the understanding of the complex problem of the oil well of Haoud Berkaoui is essential for its possible control. Modeling the case of Haoud Berkaoui, a rare and perhaps unique case in the world, will make it possible to better understand this phenomenon and to theoretically predict the areas of potential disruption in the region and to act effectively in the context of behavior monitoring and the evolution of this delicate problem, especially as its direct resolution is made impossible because of the existence of large and deep cracks around the big hole that put the life of potential stakeholders in danger of death.

The work done at the Laboratory of Physics of Materials at the School and Observatory of Physics of the Globe of Strasbourg (IPGS) consisted essentially of the modeling of the elastic deformation in an infinite plate, pierced with a hole this in order to examine the mechanical relation between the loading of the hole and the process of rupture.

Computer programming has consisted of studying the case where the cavity is loaded uniformly or non-uniformly. During the dissolution of the sodium chloride in the cavity, the latter deforms elastically, resulting in a change in displacement fields and constraints including the surface of the Earth.

This programming is based on the regular distribution of measurement stations of the stress fields and displacements on the surface of the Earth, the cutting of the contour of the cavity into segments and for each segment the calculation of the normal and tangential stresses in each station. The surface. Then we sum the effects of all the segments of the cavity and we trace the curves of stresses and displacements on the surface.

The effects of all the segments of the cavity are then summed and the stress and displacement curves are plotted on the surface. For more accurate results (real, accurate and up-to-date problem data is needed), it is necessary to use the iteration method (successive overlays), a method based on the readjustments of constraints while respecting the initial boundary conditions. This method takes into account the interaction between the free surface and the underground hole. We proceed by successive overlays until the corrective fields on the free surface and the hole are negligible.

As a preventive measure, studies have been carried out (Mellak. A., Baudeau, P., 1994), (Mellak, A., Bekkour, K., 1997); (Mellak, A., 2000) to avoid the technical faults that led to the formation of a gigantic underground cave and a major surface collapse, in other words, the formation of other Haoud Berkaoui in Algeria or elsewhere.

References

[1] Jaeger, J. C. – Cook, N. G. W. (1979): Fundamentals of rock mechanics, 3rd ed., Chapman and Hall, London.

[2] Stephenson, A. (1982): Landolt - Börnstein - Numeral data and functional relationships in science and technology, *Volume 1: Physical properties of rocks*, G. Angenheister Ed., Springer-Verlag, Berlin.

[3] Mellak, A. – Reuschlé, T. – Gueguen, Y. (1990): Mécanique de la rupture, modélisation de Haoud Berkaoui. *Rapport du D.E.A. Mécanique et Acoustique - Ecole et Observatoire de Physique du Globe de Strasbourg.*

[4] Mellak, A. – Baudeau, P. (1994): Propriétés physico-chimiques des coulis de ciment saumurés et microsilicés appropriés aux formations salifères in Annales de l'Institut Technique du Bâtiment et des Travaux Publics - Paris, n° 526, pp. 70-86.

[5] Mellak, A. – Bekkour, K. (1997): Comportement rhéologique des coulis de ciment saumurés in 13ème Congrès Français de Mécanique, Poitiers Futuroscope, pp. 397-400.

[6] Mellak, A. (2000): Environmental geology: major collapse risk in an oil-bearing region, *in Fifth International Conference on the Geology of the Arab World GAW-5*, February 21-24, 2000 of Faculty of science, Cairo University - Egypt.

[7] Muskhelishvili, N. I. (1977): Some basic of the mathematical theory of elasticity, 4th Ed., *Noordhoff International Publishing*, Leyden, The Netherlands.

[8] Pollard, D. D. – Holzhauzen, G. (1979): Mechanical interaction between a fluid-filled fracture and the Earth's surface, *Tectonophysics*, Vol. 53, pp. 27-57. https://doi.org/10.1016/0040-1951(79)90353-6

[9] Reuschlé, T. (1979) Les fluides et l'évolution des propriétés mécaniques des roches. Doctorat de l'université Louis Pasteur de Strasbourg.

[10] Mellak, A. (2017): From Nuclear to Cogeneration – How a natural disaster can change the policy of a country, *Építőanyag - Journal of Silicate Based and Composite Materials*, Vol.69, No.4, pp. 114-115. https://doi.org/10.14382/epitoanyag-jsbcm.2017.20

Ref.:
Mellak, Abderrahmane: *Mathematical modelling: case of Haoud Berkaoui*
Építőanyag – Journal of Silicate Based and Composite Materials, Vol. 71, No. 1 (2019), 12–16. p.
https://doi.org/10.14382/epitoanyag-jsbcm.2019.3

european powder metallurgy association

THE EUROPEAN POWDER METALLUGY ASSOCIATION

EPMA – Working to Promote PM

The European Powder Metallurgy Association (EPMA) was formed in Brussels in 1989, and has three key missions:

- To Promote and Develop PM Technology in Europe
- To Represent the European PM Industry within Europe and Internationally
- To Develop the Future of PM

These are achieved using a variety of means, a selection of which are described on the EPMA Activities page. We at the EPMA serve all types of member organisations; from component, metal powder, and equipment producers to end-users, research centres, universities, and individuals who have an interest in PM.

www.epma.com

Fresh properties of the self-compacting high-performance concrete using recycled concrete aggregate

Mohammed ABED ▪ Department of Construction Materials and Technologies, Budapest University of Technology and Economics, Hungary ▪ abed.mohammed@epito.bme.hu

Rita NEMES ▪ Department of Construction Materials and Technologies, Budapest University of Technology and Economics, Hungary ▪ nemes.rita@epito.bme.hu

Érkezett: 2018. 10. 06. ▪ Received: 06. 10. 2018. ▪ https://doi.org/10.14382/epitoanyag-jsbcm.2019.4

Abstract

The present study is investigating the fresh properties of the self-compacting high-performance concrete (SCHPC) using recycled concrete aggregate and waste powder materials. Twenty-one mixtures with the same water to binder ration have been tested for both slump flow and V-funnel tests. Their results shows that using recycled concrete aggregate (RCA) up to 50% is not affecting the workability of SCHPC if the water absorption of RCA is compensated, however, waste powder materials are affecting the fresh properties negatively and demanded higher dosage of chemical admixture. Their effect differentiates depending on the grading and particles properties of the waste powder material. The workability results of SCHPC using recycled aggregate and waste powder materials are satisfying the workability process of normal SCC, which is specified in the European Guideline for Self-compacting Concrete regulations (EFNARC).

Keywords: self-compacting high-performance concrete – SCHPC, recycled concrete aggregate - RCA, workability process, high range water reducing admixture – HRWRA.

Kulcsszavak: öntömörödő beton, újrahasznosított beton, nagyszilárdságú beton, bedolgozhatóság, frissbeton jellemzők, adalékszerek

Mohammed ABED

Civil engineer (MSc). PhD candidate at the Department of Construction Materials and Technologies, Budapest University of Technology and Economics. Main fields of interests: recycled concrete aggregate, non-destructive testing of concrete, high performance concrete, supplementary cementations materials, fire resistance, self-compacting concrete. Member of the Hungarian Group of fib and the Scientific Society of Silicate Industry.

Rita NEMES

Civil engineer (MSc), postgraduate degree in concrete technology, PhD, associate professor at the Department of Construction Materials and Technologies, Budapest University of Technology and Economics. Main fields of interest: concrete technology, ceramics, non-destructive testing of concrete, supplementary cementing materials for concrete, bond in concrete, fibre reinforced concrete, lightweight concrete, shrinkage of concrete, durability measurement, waste materials as aggregates. Member of the Hungarian Group of fib and the Scientific Society of Silicate Industry.

1. Introduction

It was revealed that the using of recycled concrete aggregate (RCA) affects the workability of fresh concrete negatively, where recycled aggregate concrete (RAC) has higher slump loss than the natural aggregate (NA) concrete [1-3], which is mainly due to the aggregate itself where the size, texture, shape and water content of aggregate have a high effect on the fresh priorities [4-6]. Fresh properties or workability defined in ACI as that property of freshly mixed concrete or mortar that determines the ease with which it can be mixed, placed, consolidated, and finished to a homogenous condition [7]. It is the basic property that characterizes the SCC, and to be SCC it has to flow and consolidate within the formwork without vibration and just under its own weight. Low water to binder (w/b) ratio is required in case of the self-compacting high-performance concrete (SCHPC); to achieve higher durability abilities. Thus chemical admixtures are recommended through the literature to use for enhancing the fresh properties of RAC with saving the hardened properties [5, 8, 9]. It is also recommended in the literature to use RCA with a saturated surface dry condition for enhancing the workability [10], however, using RCA at the partially wet condition or whatever its water content in the field could simulate more precisely the reality and make the study more reliable.

2. Fresh properties testing

Filling ability, passing ability, viscosity, and segregation resistance are the key primary fresh properties of the SCHPC which must be taken into consideration in the design phase of the SCHPC. Slump flow and V-funnel are the two tests were used in the present study to evaluate the properties SCHPC in addition to the physical observations. They applied in accordance with European Guideline for Self-compacting Concrete EFNARC (2005) [11], which specifies their required specifications, limitation, and classifications.

2.1 Filling ability

EFNARC (2002) [12], defined the filling ability as the ability of fresh concrete to flow into and fill all spaces within the formwork, under its own weight which absolutely fill the framework without using any means of consolidation like the vibrator. Aggregate content, aggregate size, w/b ratio, binder content, binder type and HRWR dosage of concrete are the main factors affecting the filing ability [13, 14]. Where getting better filling ability could be achieved by:

- Using the optimal dosage of high range water reducing admixture (HRWR), which is neither too much to avoid segregations nor less the required to control the rheological parameters and reduce the yield stress and plastic viscosity.
- Using cementing materials enhance the segregation resistance, which improves the filling ability, the cementing materials could be filler materials or supplementary cementitious materials (SCMs), where the waste powder materials could be achieved the properties of the filling materials or SCMs [15].

Wherein case of using RCA the focus on other enhancing parameters should be of high importance. *Table 1* summarizes the slump flow classes, which is related to the flowability and filling ability in unconfined conditions.

Slump flow classes	Mean slump flow diameter (mm)
SF1	550 – 650
SF2	660 – 750
SF3	760 – 850

Table 1 The slump flow classes by EFNARC (2005) [11]
1. táblázat Terülési osztályok az EFNARC (2005) szerint [11]

2.2 Segregation resistance

The ability of concrete to remain uniform during and after placement without any loss of stability due to bleeding, mortar separation and coarse aggregate settlement is the segregation resistance [12]. Choosing better grading of aggregates, decreasing the maximum aggregate size, using cementing materials with cement, and decreasing the w/b ratio enhances the segregation resistance [16, 17], where in case of SCHPC the low segregation resistance decrease the durability of concrete [18].

Segregating resistance could be investigated by physical inspection through the test of slump flow and casting of concrete, where the lack of any bleeding or separation is good induction for good resistance of segregation. However, the passing ability which is defined at EFNARC (2002) as the ability of fresh SCHPC to flow through tight openings or spaces confined by steel reinforcing bars, could be achieved as well by limiting the segregation of coarse aggregate.

2.3 Viscosity

The resistance to the flow of concrete once flow has started is the definition of the viscosity of concrete, which could be determined by investigating the efflux time in the V-funnel test [11]. The flow time has to be limited to be from 6 to 12 second by using the V-funnel test to achieve the good viscosity of SCHPC. Where the concrete with a low viscosity will have a very quick initial flow and then stop, while the concrete with a high viscosity may continue to creep forward over an extended time [11, 12].

2.4 Processing window

Processing window is a window created by mainly two coordinates, those coordinates are the slump flow (mm) in the x-axis and V-funnel time (s) in the y-axis, which could help to assess and limits the targeted values based on the upper and lower limits of the slump flow and for the V-funnel time tests. Some modifications have been suggested on the limited ranges EFNARC by a number of researchers who they investigated the fresh properties of SCHPC [16, 17]. However, in the present study the suggested window EFNARC tested for its applicability in case of using RCA in the SCHPC.

3. Experimental method

Twenty-one mixtures of SCHPC have been designed to achieve the properties of SCC at the fresh stage, 500 kg/m^3 binder content, and a 0.35 w/b ratio were constant throughout this experimental study. The variables through the present study were the aggregate and the binder type, where the coarse NA have been replaced partially (25% or 50%) by RCA, and the cement has been replaced partially (15% or 30%) by three different waste powder materials. The used cement was a pure Portland cement CEM I 42.5 N, where the waste powder materials were:

- Unprocessed waste fly ash (UWFA) which collected from a coal power station in Hungary (Visonta coal-fired thermal power station) and delivered to the laboratory for use in the testing program without any processing.
- Waste cellular concrete powder (WCCP) which is a waste material collected from a factory for cutting cellular concrete masonry in Hungary.
- Waste perlite powder (WPP) which is amorphous volcanic silicate/alumina rock which originating from raw perlite resulting from cutting the raw perlite rock, where Hungary consider one of the main countries for producing Perlite [19]. *Fig. 1* shows the sieve curves for both cement and waste powder materials.

The NA used in the present study was quartz sand and gravel (0/16 mm size), which have been imported with three nominal grading fractions, sand (0/4 mm), small gravel (4/8 mm), medium gravel (8/16 mm), where divided regarding the fractions to 45%, 30%, and 25% respectively. While the coarse RCA fraction (4/16 mm size) produced by crushing of concrete cubes with average compressive strength between 28 to 33 MPa. The particle grading distribution shown in *Fig. 2*.

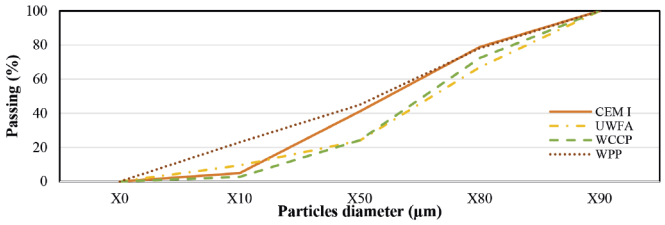

Fig. 1. Grading curves of cement and waste materials
1. ábra A cement és a hulladékporok szemmegoszlási görbéje

A considerable amount of HRWRA was required to achieve the deformability and resistance to segregation at fresh state. Sika ViscoCrete-5 Neu is a modified polycarboxylates aqueous solution, which has been used as HRWRA in the present study to achieve and ensure the rheological properties of the fresh SCC.

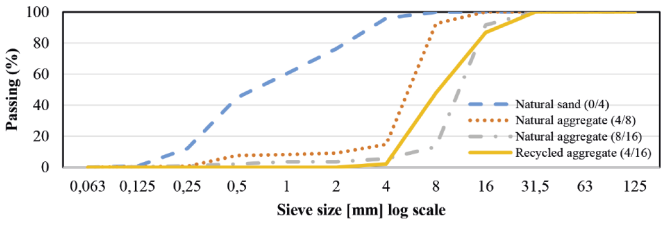

Fig. 2. Grading curves of different types of aggregates
2. ábra A különböző adalékanyagok szemmegoszlási görbéje

Replacement of cement	Series I 0% replacement of coarse aggregate with RA	Series II 25% replacement of coarse aggregate with RA	Series III 50% replacement of coarse aggregate with RA
0%	RA0	RA25	RA50
15% UWFA	F15RA0	F15RA25	F15RA50
30% UWFA	F30RA0	F30RA25	F30RA50
15% WCCP	C15RA0	C15RA25	C15RA50
30% WCCP	C30RA0	C30RA25	C30RA50
15% WPP	P15RA0	P15RA25	P15RA50
30% WPP	P30RA0	P30RA25	P30RA50

Table 2. Mixing series
2. táblázat Keverési sorozatok

Name of mixture	Proportions in kg/m³						
	CEM I 42.5 N	Waste material	Fine aggregate	Coarse aggregate		Superplasticizer	Water
			N. Sand	NA	RCA		
			0/4	4/16			
Series I							
RA0	500	0	783	939	0	1.5	175
RA25	500	0	783	704	230	1.5	175
RA50	500	0	783	470	460	1.5	175
Series II							
F15RA0	425	75	767	920	0	2	175
F15RA25	425	75	767	690	226	2	175
F15RA50	425	75	767	460	251	2	175
Series III							
F30RA0	350	150	751	901	0	3	175
F30RA25	350	150	751	475	221	3	175
F30RA50	350	150	751	451	442	3	175
Series IV							
C15RA0	425	75	766	919	0	1.7	175
C15RA25	425	75	766	690	225	1.7	175
C15RA50	425	75	766	459	451	1.7	175
Series V							
C30RA0	350	150	750	899	0	3.25	175
C30RA25	350	150	750	674	220	3.25	175
C30RA50	350	150	750	451	442	3.25	175
Series VI							
P15RA0	425	75	774	928	0	3	175
P15RA25	425	75	774	697	228	3	175
P15RA50	425	75	774	464	455	3	175
Series VII							
P30RA0	350	150	766	918	0	3.75	175
P30RA25	350	150	766	688	225	3.75	175
P30RA50	350	150	766	459	450	3.75	175

Table 3. Concrete mixing proportioning
3. táblázat A betonkeverékek összetétele

The twenty-one mixtures were allocated through seven series; each series contains three mixtures with the same type of binder and amount of HRWR to investigate the actual effect of each replacement amount of both RCA and waste powder materials on the fresh properties of SCHPC. *Table 2* shows the produced mixtures for the present study, while *Table 3* shows the chemical compositions for all mixture. Where mainly two replacement amounts of NA have been replaced by RCA (25% and 50%) while the cement has been replaced by two percentages by each of the proposed waste powder materials (15% and 30%).

4. Mixing procedure

Mixing was carried out in accordance with EN 196-1 [20] for a total mixing time of four and a half minutes partitioned in three stages by using an electric concrete mixer. After each stage, the ingredients were manually mixed to achieve the highest homogeneity. The first stage the aggregate and binder powders are mixed, the second stage the water is added, and finally in the third stage the HRWR is added. The samples have been cast in steel molds having different sizes to obtain the standard specimens for each test. The fresh properties have been tested after one minute of finishing the mixing, which means after 4 minutes from adding water. The mixing procedure has a significant effect on both fresh and hardened concrete, in the present study the mixing procedure have been optimized as the first step for the study.

5. Results

5.1 High range water reducer demand

To achieve the European Guideline for Self-compacting Concrete regulations and to study the countless effects of RCA, UWFA, WCCP, and WPP, the adding amount of HRWR have been optimized in the preparation stage. *Fig. 4* shows the HRWR demand in case of using the waste powder materials with and without RCA, where using RCA up to 50% does not affect the fresh properties of SCHPC. In RAC mixtures the water absorption capacity of RCA was compensated, which in this case almost the same slump flow (between 67.5 to 69.75 cm) and flow time (between 6 to 12 s) have been recorded by using the same amount of HRWR as shown in *Fig. 4* at point (a). However, the water absorption capacity of the adhered mortar in RCA is the main reason which affects the workability of RAC but by compensating the water absorption the negative effect of RCA on workability could be eliminated despite that the effect of the rough surface of RCA will still slightly affects the flow time of RAC.

Where the literature is not discussing the three of the previously mentioned waste powder materials and their effect on the fresh properties of SCHPC, where in this case the demand of HRWR has been optimized in form of a linear relationship for each waste powder material at constant binder content 500 kg/m³. The demand of HRWR increased linearly by increasing the dosage of waste powder materials, due to the absorption capacity and different grading fraction comparing to the cement.

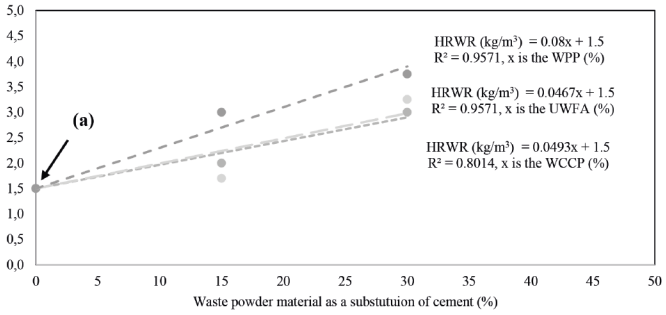

Fig. 4. The HRWR demand by increasing the waste powder materials substitution
4. ábra A cementhelyettesítések hatása a folyósítószer-igényre különböző hulladékporok esetén

In case of using any of the three waste powder materials the concrete mixtures demanded HRWR with a linear function ($R^2 > 0.83$), however, in case of using the three of the waste powder materials together with the same amounts, the demanded HRWR was in a linear function for the average dosage of the dosages whom using for each alone. The function is:

$$HRWR\ (kg/m^3) = 0.0585x + 1.5,$$

where x is equal to the total substitution of cement by waste powder materials in percentage (%), when the three of the waste powder materials are using together with the same equal amounts. This function has been gotten by optimizing two mixes with the three of waste powder materials together for achieving the requirements of European guideline EFNARC (2005), where the first mix was with replacing 15% of cement by waste powder materials (5% UWFA + 5%WCCP +5%WPP), while the second by 10% for each. *Fig. 5* shows the HRWR demand by increasing the dosage of waste powder materials, in case of using the three of the waste powder materials together with the same dosage of each.

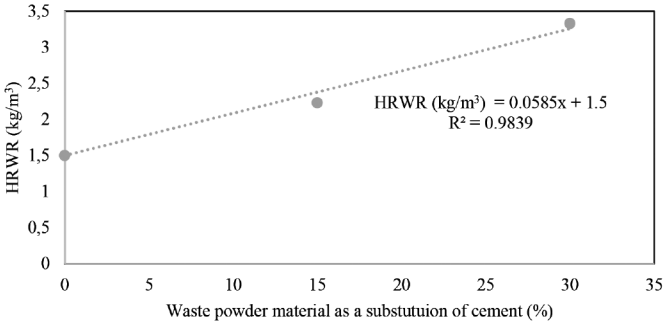

Fig. 5. The HRWR demand by increasing waste powder materials substitution, (in case of using the three of the waste powder materials together with the same dosage of each)
5. ábra A cementhelyettesítések hatása a folyósítószer-igényre a különböző hulladékporok együttes használatával (mindhárom azonos mennyiségben való alkalmazása esetén)

5.2 Slump flow and V-funnel

Increasing the amount of RCA decreases the slump diameter slightly which agrees with most researchers findings [21-23], as well as the flow time has increased by adding 50% of RCA and that is mainly related to the shape and texture of RCA compared with the NA that have been used. While the RCA has greater surface roughness and relatively big amount fine particles, which were a result of the processes of crushing, these factors affect the slump diameter and the flow time of the mixtures directly against increasing the amount of the involved RCA.

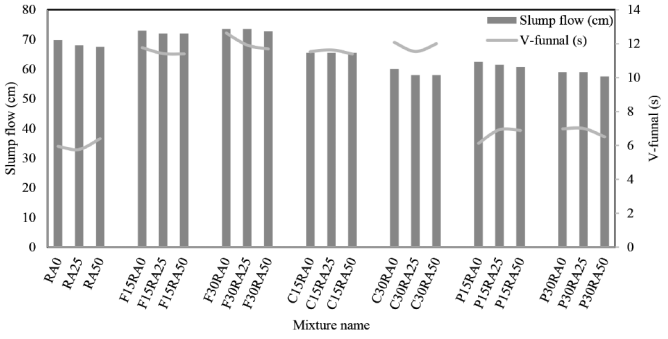

Fig. 6. Results of slump and V-funnel tests
6. ábra A terülés a kifolyási idő vizsgálatának eredményei

Fig. 6 shows the results of slump flow and V-funnel tests for all mixtures and series. It is clear that adding UWFA as a replacement of cement either by 15 or 30% cause decreasing in the slum flow even by using a higher amount of HRWR. This behavior might be due to the big particles and the high-unburned carbon content of the added UWFA, where these two parameters absorb higher amount of water, resulting in less workability [24, 25]. Almost the same behavior has been observed by adding WCCP, which also has relatively big particles size compared to cement, in addition to its ability to absorb a high amount of water. Despite the slump, flow and V-funnel time are not changed significantly by adding WPP; the fresh properties considered as negatively affected when WPP added for both recycled and natural aggregate concrete. Where the required amounts of superplasticizer have been increased considerably, this reduction in workability might be due to the high surface area of WPP and its absorption capacity [26, 27]. The WPP does not affect the V-funnel time because WPP consumes longer time to absorb water due to its special amorphous, as well as its particles are relatively small comparing to UWFA and WCCP.

The effect of RCA was ranged in less than 30 mm concerning flow diameter and 1.5 seconds concerning flow time, which its effect could be neglected and that due to compensating of the water absorption capacity of RCA by adding water for RAC mixtures. However, by increasing the amount of any of the waste powder materials; the flow time increase and that is due to amorphousness and water absorption capability of the waste powder materials if compared with ordinary Portland cement (OPC) especially in case of using UWFA. That does not agree with SCHPC incorporating processed fly ash where the flowability increase in that situation [28]. All of the obtained measures of slump flow and V-funnel tests throughout all series satisfied the European guideline EFNARC (2005) and the suggested determinations of the previous literature.

5.3 Processing window

The workability ranges for all SCHPC mixtures shows the same rang of EFNARC (2002) regulation for normal SCC, which indicate that the EFNARC regulations for SCC are

also appropriate for SCHPC either by using NA or RCA. Where those regulations have been proposed by EFNARC to avoid any segregations or stagnations. *Fig. 7* shows that the processing window of SCHPC mixtures, which is the same as the recommended processing window by EFNARC (2002) regulation for SCC.

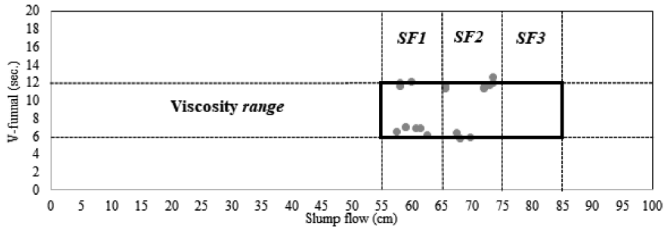

Fig. 7. Processing window of RASCC
7. ábra Alkalmazhatósági tartomány hulladék adalékanyagos öntömörödő betonok esetén

The visual examination was carried out during mixing and by inspection the periphery of the concrete after measuring the slump flow, where no segregations or agglomerations of aggregate have been observed as well as the amount of HRWR optimized to produce a healthy mixture with appropriate fresh properties.

6. Conclusions

The present study is investigated the fresh properties of the self-compacting high-performance concrete (SCHPC) using recycled concrete aggregate (RCA) and waste powder materials. Where the main conclusions that could be concluded are:

- RCA does not affect the fresh properties of SCHPC significantly if the water absorption of RCA is compensated, whereby adding waste powder materials the effect decrease more,
- Waste powder materials affect the fresh properties of SCHPC negatively in both cases of using either NA or RCA,
- The demand of HRWR increase by increasing the replacement amount of cement by any of the waste powder materials.
- The workability process window of SCHPC using recycled aggregate is satisfying the workability process of normal SCC which is specified in the European Guideline for Self-compacting Concrete regulations (EFNARC),
- Slump flow and V-funnel tests with the physical observations are very important to produce and classify the fresh properties of SCHPC.

6. Acknowledgments

Authors are grateful to the Hungarian Scientific Research Fund (OTKA) for the financial support of the OTKA K 109233 research project. Special thanks to Duna-Dráva Cement Kft., SIKA Hungária Kft. for providing the materials used in the experiments.

References

[1] Debieb, F. – Courard, L. – Kenai, S. – Degeimbre, R. (2009): Roller compacted concrete with contaminated recycled aggregates. *Construction and Building Materials*, Vol. 23, No. 11, pp. 3382-3387. https://doi.org/10.1016/j.conbuildmat.2009.06.031

[2] Hama, S. M. – Hilal, N. N. (2017): Fresh properties of self-compacting concrete with plastic waste as partial replacement of sand. *International Journal of Sustainable Built Environment,* Vol. 6, No. 2, pp. 299-308. https://doi.org/10.1016/j.ijsbe.2017.01.001

[3] Carro-López, D. – González-Fonteboa, B. – Martínez-Abella, F. – González-Taboada, I. – Brito, J. – Varela-Puga, F. (2017): Proportioning, Microstructure and Fresh Properties of Self-compacting Concrete with Recycled Sand. *Procedia Engineering,* Vol. 171, pp. 645-657. https://doi.org/10.1016/j.proeng.2017.01.401

[4] Kou, S. C. – Poon, C. S. (2009): Properties of self-compacting concrete prepared with coarse and fine recycled concrete aggregates. *Cement and Concrete Composites,* Vol. 31, No. 9, pp. 622-627. https://doi.org/10.1016/j.cemconcomp.2009.06.005

[5] Revathi, P. – Selvi, R. S. – Velin, S. S. (2013): Investigations on Fresh and Hardened Properties of Recycled Aggregate Self Compacting Concrete. *Journal of The Institution of Engineers (India): Series* A, Vol. 94, No. 3, pp. 179-185. https://doi.org/10.1007/s40030-014-0051-5

[6] Revathi, P. – Mani, S. (2014): Studies on Fresh and Hardened Properties of Recycled Aggregate Concrete with Quarry Dust. *ACI Materials Journal,* Vol. 111. pp. 283-289. https://doi.org/10.14359/51686507

[7] CT-13: ACI Concrete Terminology - An ACI Standard 2013.

[8] Kisku, N. – Joshi, H. – Ansari, M. – Panda, S. K. – Nayak, S. – Chandra Dutta, S. (2017): A critical review and assessment for usage of recycled aggregate as sustainable construction material. *Construction and Building Materials,* Vol. 131, pp. 721-740. https://doi.org/10.1016/j.conbuildmat.2016.11.029

[9] Madandoust, R. – Mousavi, S. Y. (2012): Fresh and hardened properties of self-compacting concrete containing metakaolin. *Construction and Building Materials,* Vol. 35, pp. 752-760. https://doi.org/10.1016/j.conbuildmat.2012.04.109

[10] Yong, P. C. – Teo, D. C. L. (2009): Utilisation of Recycled Aggregate as Coarse Aggregate in Concrete. *Journal of Civil Engineering, Science and Technology,* Vol. 1, No. 1

[11] EFNARC, Specifications and guidelines for self-compacting concrete, English ed. *European federation for specialist construction chemicals &concrete systems*, 2005.

[12] EFNARC, Specifications and guidelines for self-compacting concrete, English ed. 2002, *European federation for specialist construction chemicals &concrete systems.*

[13] Puthipad, N. – Ouchi, M. – Rath, S. – Attachaiyawuth, A. (2016): Enhancement in self-compatibility and stability in volume of entrained air in self-compacting concrete with high volume fly ash. *Construction and Building Materials,* Vol. 128, pp. 349-360. https://doi.org/10.1016/j.conbuildmat.2016.10.087

[14] Megat Johari, M. A. – Brooks, J. J. – Kabira, S. – Rivard, P. (2011): Influence of supplementary cementitious materials on engineering properties of high strength concrete. *Construction and Building Materials,* Vol. 25, No. 5, pp. 2639-2648. https://doi.org/10.1016/j.conbuildmat.2010.12.013

[15] Mehmet Karatas, A. G. (2015): Engineering Properties of Self-Compacting Concrete Produced by Polypropylene and Steel Fiber. *Periodica Polytechnica Civil Engineering,* Vol. 59, No. 2, pp. 95-102.

[16] Güneyisi, E. – Gesoglu, M. – Al-Rawi, S. – Mermerdas, K. (2013): Effect of volcanic pumice powder on the fresh properties of self-compacting concretes with and without silica fume. *Materials and Structures,* Vol. 47. https://doi.org/10.1617/s11527-013-0155-9

[17] El Mir, A. – Nehme, S. G. (2017): Assessment of the fresh selfcompacting concrete properties utilizing different types of additives. Építőanyag, *Journal of Silicate Based and Composite Materials,* Vol. 69, No. 3, pp. 83-88. https://doi.org/10.14382/epitoanyag-jsbcm.2017.14

[18] Assaad, J. – Khayat, K. – Daczko, J. (2004): Evaluation of Static Stability of Self-Consolidating Concrete. *ACI Materials Journal,* Vol. 101, pp. 168-176.

[19] Rashad, A. M. (2016): A synopsis about perlite as building material – A best practice guide for Civil Engineer. *Construction and Building Materials,* Vol. 121, pp. 338-353. https://doi.org/10.1016/j.conbuildmat.2016.06.001

[20] EN 196-1: Methods of testing cement. Determination of strength 2016.
[21] Omrane, M. – Kenai, S. – Kadri, E-H. – Ait-Mokhtar, A. (2017): Performance and durability of self compacting concrete using recycled concrete aggregates and natural pozzolan. *Journal of Cleaner Production,* Vol. 165, pp. 415-430. https://doi.org/10.1016/j.jclepro.2017.07.139
[22] Safiuddin, M. D. – Salam, M. A. – Jumaat, M. Z. (2011): Effects of recycled concrete aggregate on the fresh properties of self-consolidating concrete. *Archives of Civil and Mechanical Engineering,* 2011. Vol. 11, No. 4, pp. 1023-1041. https://doi.org/10.1016/S1644-9665(12)60093-4
[23] Silva, Y. F. – Robayo, R. A. – Mattey, P. E. – Delvasto, S. (2016): Properties of self-compacting concrete on fresh and hardened with residue of masonry and recycled concrete. *Construction and Building Materials,* Vol. 124, pp. 639-644. https://doi.org/10.1016/j.conbuildmat.2016.07.057
[24] Snelson, D. G. – Kinuthia, J. M. (2010): Characterisation of an unprocessed landfill ash for application in concrete. *Journal of Environmental Management,* Vol. 91, No. 11, pp. 2117-2125. https://doi.org/10.1016/j.jenvman.2010.04.015
[25] Hamood, A. – Khatib, J. M. – Williams, C. (2017): The effectiveness of using Raw Sewage Sludge (RSS) as a water replacement in cement mortar mixes containing Unprocessed Fly Ash (u-FA). *Construction and Building Materials,* Vol. 147, pp. 27-34. https://doi.org/10.1016/j.conbuildmat.2017.04.159
[26] Karein, S. M. M. – Joshaghani, A. – Ramezanianpour, A. A. – Isapour, S. – Karakouzian, M. (2018): Effects of the mechanical milling method on transport properties of self-compacting concrete containing perlite powder as a supplementary cementitious material. *Construction and Building Materials,* Vol. 172, pp. 677-684. https://doi.org/10.1016/j.conbuildmat.2018.03.205
[27] El Mir, A. – Nehme, S. G. (2017): Utilization of industrial waste perlite powder in self-compacting concrete. *Journal of Cleaner Production,* Vol. 156, pp. 507-517. https://doi.org/10.1016/j.jclepro.2017.04.103
[28] Sabet, F. A. – Libre, N. A. – Shekarchi, M. (2013): Mechanical and durability properties of self consolidating high performance concrete incorporating natural zeolite, silica fume and fly ash. *Construction and Building Materials,* Vol. 44, pp. 175-184. https://doi.org/10.1016/j.conbuildmat.2013.02.069

Nagyszilárdságú öntömörödő beton frissbeton jellemzői hulladék anyagok hasznosításával Öntömörödő, nagy teljesítőképességű betonok (SCHPC) frissbeton jellemzőit vizsgáltuk újrahasznosított beton adalékanyagként való felhasználásával és különböző hulladékalapú (feldolgozatlan pernye, perlit, pórusbetonpor) cementhelyettesítő, illetve kiegészítő anyagok alkalmazása esetén. Huszonegy keveréket vizsgáltunk, a terülést és a kifolyási időt mérve. Eredményeik azt mutatják, hogy a kavicsfrakció 25 és 50%-os helyettesítése újrahasznosított betonzúzalékkal (RCA) nem rontja az SCHPC bedolgozhatóságát, ha a betonzúzalék vízfelvételét számításba vesszük. A hulladékalapú cementhelyettesítő anyagok viszont negatívan befolyásolják a friss tulajdonságokat, és jelentősen megnő a folyósítószer-igény, de megfelelő keverékek esetén újrahasznosított adalékanyagok és hulladék alapú kiegészítő anyagok együttesen is alkalmazhatók úgy, hogy az öntömörödő betonokra vonatkozó elvárásoknak (EFNARC) megfeleljen.
Kulcsszavak: öntömörödő beton, újrahasznosított beton, nagyszilárdságú beton, bedolgozhatóság, frissbeton jellemzők, adalékszerek

Ref.:
Abed, Mohammed – **Nemes,** Rita: *Fresh properties of the self-compacting high-performance concrete using recycled concrete aggregate*
Építőanyag – Journal of Silicate Based and Composite Materials, Vol. 71, No. 1 (2019), 18–23. p.
https://doi.org/10.14382/epitoanyag-jsbcm.2019.4

Upper Ludlowian-lower Pridolian stratigraphy, carbon isotope of the Timan-Northern Urals region

Tatiana M. BEZNOSOVA ▪ Institute of Geology Komi SC UB RAS, Syktyvkar ▪ beznosova@geo.komisc.ru
Vladimir A. MATVEEV ▪ Institute of Geology Komi SC UB RAS, Syktyvkar ▪ vamatveev@geo.komisc.ru
Lioubov V. SOKOLOVA ▪ Institute of Geology Komi SC UB RAS, Syktyvkar ▪ sokolova@geo.komisc.ru
Érkezett: 2018. 10. 11. ▪ Received: 11. 10. 2018. ▪ https://doi.org/10.14382/epitoanyag-jsbcm.2019.xx

Abstract
The paper presents the results of studying the geological structure of the Ludlowian boundary sediments and data on lithology, bio- and chemostratigraphy, and large-scale biotic reconstruction at the boundary Ludlow-Pridoli. The results obtained make it possible to draw a conclusion about the stratigraphic incompleteness of the Ludlow section in the Subpolar Urals and the interruption in sedimentation at the end of the Ludlow.
Keywords: brachiopods, ostracods, conodonts, Silurian, carbon isotope, events, boundary Ludlow-Pridoli, Timan-Northern Urals region, Russia
Kulcsszavak: pörgekarúak, kagylósrákok, konodonták, szilúri, karbon izotóp események, ludlovi-pridoli határa, Timan-Észak Ural régió, Oroszország

Tatiana M. BEZNOSOVA
Leading researcher at the laboratory of stratigraphy. Works at the N.P. Yushkin institute of Geology, Komi Science Centre, Ural Division, Russian Academy of Sciences, Syktyvkar (Russian Federation). Main fields of her research interest are event stratigraphy, bio-chemostratigraphy, systematic, paleoecology and paleobiogeography brachiopods of the late Ordovician, Silurian and early Devonian Timan-Northern Urals region. She is author of 4 books and more than 150 scientific papers.

Vladimir A. MATVEEV
Scientific employee in the laboratory of stratigraphy at the n N.P. Yushkin institute of Geology of the Komi SC UB RAS. Main fields of his research interest are stromatolite constructions of the Silurian of the Western slope of the Urals and the Chernov uplift. He is author of more than 30 scientific papers.

Lioubov. V. Sokolova
Scientific employee in the laboratory of stratigraphy at the n N.P. Yushkin institute of Geology of the Komi SC UB RAS. Main fields of her research interest are biostratigraphy, systematic, paleoecology of the Silurian conodont Timan-Northern Urals region. She is author of more than 30 scientific papers.

1. Introduction

The evolutionary replacement of the brachiopods Didymothyris didyma (Dalman) and the Collarothyris canaliculata (Wenjukov), and the renewal of the taxonomic composition and a significant increase in the diversity of the biota observed in the characteristic lumpy limestones that form the bottoms of the Belush'ya stage of the Pridoli, is the basis of the paleontological study of the boundary Ludlow-Pridoli in Severouralsk region. The boundary Ludlow-Pridoli was adopted at the base of these lumpy limestones of the Belush'ya stage, in which the terrigenous or terrigenous-carbonate member is universally distinguishable, as reflected in the Ural stratigraphic scheme [1].

It should be noted that there is another point of view on the position of the boundary Ludlow-Pridoli in the Ural cuts, according to which this boundary lies above the carbonate-terrigenous member, in the thickness of the lumpy limestones of the Belush'ya stage of the Pridoli [2].

The results of the newly conducted study of the boundary layers of the Ludlow-Pridoli in the Upper Silurian base section on the western slope of the Subpolar Urals, during which the previously unknown interval of the 16 m cut was uncovered, allow us to conclude that there is a break in the sedimentation that separates the Ludlow and Pridoli deposits.

The complexity of solving the problem of determining the boundary Ludlow-Pridoli in the North Urals region within the Mikhailovsky-Vaigach structural-facies zone is that the complex of brachiopods and other fauna characterizing stratotypic sections of the regional stages of Pridoli (Belush'ya and Karpov) do not contain species that are characteristic for Pridoli deposits in the global stratotype of the Czech Republic [1].

2. Geological settings

In the current structural-tectonic plan, the investigated section (236) lies within the Pre-Ural foredeep of the West Ural structural zone. Paleozoic deposits in this region belong to the Yelets (shelf) structural-formational zone and form natural outcrops, traced for more than 100 km along the right and left banks of the river Kozhym, and are confined to the periclinal closure of the Obeiz anticline (latitude 65°40'0.86"C, longitude 59°45'2.09"B) [3, 4].

3. Materials and methods

The interval of 24 m boundary Ludlow-Pridoli deposits considered here, in the terrigenous-carbonate section (236), chosen as the reference for the whole of the European North-East of Russia, is located on the western slope of the Subpolar Urals, on the Kozhym river (*Fig. 1*). The biostratigraphic separation of the Upper Silurian deposits in the Severouralsk region is based primarily on the zonal scale for brachiopods. Zonal dominant species have the narrowest stratigraphic and wide lateral ranges of distribution in Severouralsk region and beyond it (*Fig. 2*) [5].

The material for the article was presented by the authors' previously published brachiopod collections from the section 236, the published definitions of ostracods studied by A.F. Abushik and conodonts studied by S.V. Melnikov [6]. The definitions of brachiopods were made by T.M. Beznosova, vertebrates - by T. Märss and conodonts - by L.V. Sokolova and P. Männik.

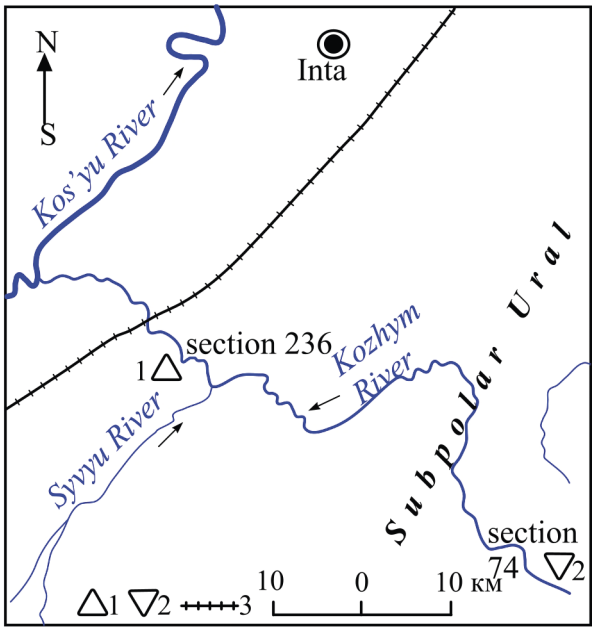

Fig. 1. Scheme of the location of the studied section in the Kozhym river basin (latitude N65°40'0.86", longitude E59°45'2.09"). Designations: (1) Polygnathoides siluricus (Branson and Mehl), (2) shell Pentamerid in the Reef Ecosystem, (3) railroad

1. ábra A vizsgált terület sémája a Kozhym folyó medencéjében (szélesség N65°40'0.86", hosszúság E59°45'2.09"). Jelölések: (1) Polygnathoides siluricus (Branson és Mehl), (2) kagylóhéj Pentamerid a zátony ökoszisztémában, (3) vasútvonal

During the field work, P. Männik and V. Matveev carried out a layer-by-layer description of the section and made new collections – more than 100 rock samples and with the remains of fossil macrofauna, 22 samples for conodonts and other microfauna, 98 samples for the isotope δ13 C_{carb}. Also, a previously uncovered interval of the Upper Ludlow section was uncovered, with a thickness of more than 16 m.

The history of the study and the significance of the results of earlier studies of this section (236), selected as a reference for the Upper Silurian of the entire territory of the European North-East of Russia, are given in of monographs [5, 6, 7].

Determination of the isotope δ13 C_{carb} in carbonate rocks was carried out at the Geonauka Center of the Institute of Geology, Komi Science Center, Uralian Division of the Russian Academy of Sciences, on the DELTA V Avantage mass-spectrometer (analyst I. V. Smoleva). The value of the isotopic coefficients was determined in ppm (‰) by the standards PDB NBS18 and NBS19 (TS-limestone) for carbon. The error in determining both coefficients did not exceed ± 0.1 ‰. The isotope δ13 C_{carb} is determined in 98 samples (a sampling step of 50 cm). All analytical works were carried out at the Institute of Geology, Komi Science Center, Uralian Division of the Russian Academy of Sciences named after academician N.P. Yushkin.

Collections are stored in the Museum of A.A. Chernov of the Institute of Geology, Komi Science Center, Uralian Division of the Russian Academy of Sciences named after Academician N.P. Yushkin (collection № 514 – lithological specimens and sections, № 368 – brachiopods, 693 – conodonts, № 654 – vertebrates).

4. Results and discussion

The late Ludlow (Ludlow) age of the Sizim stage determines the remains of the vertebrates Phlebolepis elegans Pander, pandemic conodonts Polygnathoides siluricus (Branson and Mehl) and brachiopods Didymothyris didyma (Dalman), which can be found in its sediments.

The sediments of the 15.5 m of the Upper Sizim stage are characterized by a gradual reduction in the taxonomic diversity of the biota, the disappearance of the Ludlowian brachiopods Didymothyris and the conodonts Adctenognathodus (*Fig. 2*). 10 genera of the ostracods of 18 disappear at the end of the Ludlow. The sedimentation signs of shallowing upwards along the section are clearly manifested - the alternation of limestones of stromatolitic, oolitic, microbial-clotting and dolomites with interlayers of flat-pebbled conglomerates, with cracks of desiccation, biomorphic, organogenic detritus, litho- and bioclasts with redeposited pebbles of limestone composition (*Fig. 2.A*). The maximum of the relative sea level falls on the end of the Ludlow. Reduction of the taxonomic diversity of fauna, replaced by the dominance of stromatolite-forming biota, observed in the section, indicates a major ecosystem restructuring at the end of the Ludlow (*Fig. 2.B*).

The upper boundary of the Ludlow Sizim stage was determined from the top of the interlayer of reddish-mottled clays, which fix the final regressive phase of the basin development at the end of the Ludlow and the characteristic features of the break in sedimentation (*Fig. 2.C*). [8, 9].

The transition from Ludlow to Pridoli deposits is lithologically fixed by a dolomite interlayer with large lithoclasts (break breccias, overlapping reddish-mottled clays) and thick lumpy dolomites with interbeds of calcareo-argillaceous black carbonaceous shaly mudstones corresponding to a new, transgressive sedimentation cycle. The transgression at the beginning of Pridoli facilitated the transportation and mass burial of organic matter at the base of the Belush'ya stage.

Paleontologically, this transition is characterized by a completely renewed composition of brachiopods [10] and ostracods [11]. The conodont complex of the lower part of the Belush'ya stage is mainly represented by the wide

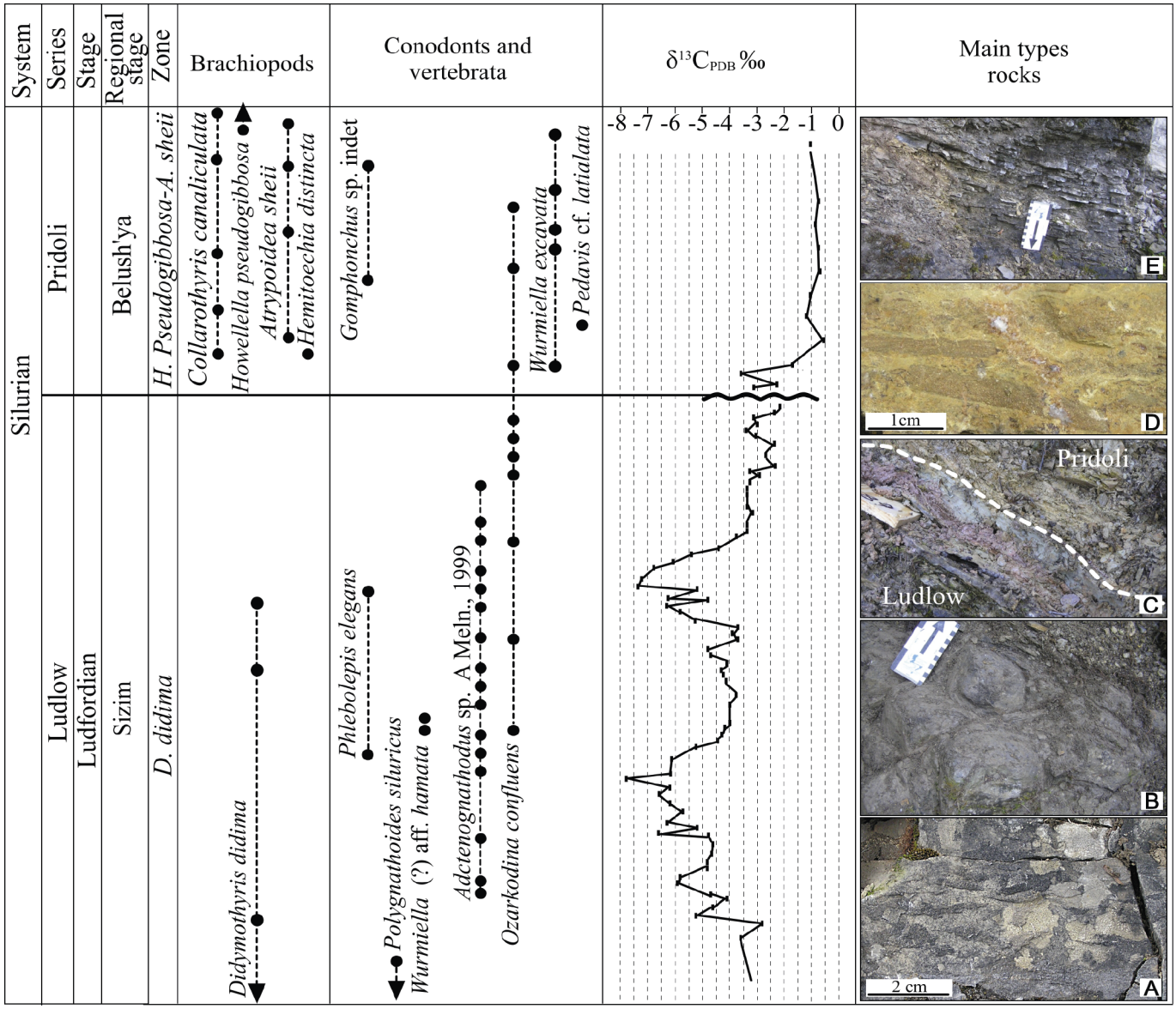

Fig. 2. Distribution of brachiopods, conodonts and vertebrates, isotopes δ13 C_{carb} and lithological features in the boundary deposits of Ludlow and Pridoli on the Western slope of the Subpolar Urals (section 236). Designations: A– dolomites with interlayers of flat-pebbled conglomerates (layer 24, Sisim stage); B– shaped stromatolite buildups (layer 64, Sisim stage); C– ludlov and pridol border (layer 68); D– interlayer with coarse material layer 68a (Belushinsky stage); E– interlayering of black carbonaceous argillites, siltstones of limestone and cloddy limestones with brachiopods Hemitoechia distincta Nikiforova and Collarothyris canaliculata (layer 72, Belushinsky stage)

2. ábra Pörgekarúak, konodonták és gerincesek, izotóp δ13 C_{carb} litológiai jellemzők a ludlovi-pridoli határán a szubpoláris Ural nyugati lejtőjén (szekció: 236). Jelölések: A– dolomitok lapos kavicsos konglomerátummal (réteg 24, Sisim stádium); B– alakos sztromatolit felépülések (réteg 64, Sisim stádium); C– ludlovi-pridoli határ (réteg 68); D– köztes réteg durva anyag réteggel 68a (Belushinsky stádium); E– köztes réteg; fekete széntartalmú agyagpalák, iszapkövek, mészkövek és rögös mészkövek pörgekarúakkal (Hemitoechia distincta Nikiforova és Collarothyris canaliculata; réteg 72, Belushinsky stádium)

geographical distribution of Wurmiella excavata (Branson and Mehl), Ozarkodina confluens (Branson and Mehl), Pedavis cf. latialata (Walliser), Oulodus cf. siluricus (Branson and Mehl), Panderodus unicostatus (Branson and Mehl) [12] (*Fig. 2*).

The Belush'ya stage of Pridoli (8.5 m) in the same section (236) in the base is composed of limestone dolomites with large lithoclasts (break breccias), oriented along the bedding of rocks (*Fig. 2.D*). Above are the limestones with intercalations of black calcareous-carbonaceous shaly mudstones and greenish-gray mudstones with the brachiopods of Hemitoechia distincta Nikiforova, which overlap limestones lumpy (*Fig. 2.E*) with brachiopods Collarothyris canaliculata (Wenjukov), Atrypoidea sheii (Holtedahl), Howellella pseudogibbosa Nikiforova [5]. This shelly layer forms distinct marking brachiopod layers in the lower part of the Belush'ya stage, which can be traced in the sections of the Subpolar and Northern Urals, on the Chernov and Chernyshev uplifts, as well as numerous wells drilled on the territory of the Timan-Pechora oil and gas province. Similar layers with a complex of brachiopods, differing only in a large variety of representatives of the genus Atrypoidea, were first described by O.I. Nikiforova from the lower stratum of Pridoli of Vaigach island [13, 14]. The complex of conodonts is represented mainly by species of wide geographical distribution and long-term existence of Wurmiella excavata (Branson and Mehl), Ozarkodina confluens (Branson and Mehl), Pedavis cf. latialata (Walliser), Oulodus cf. siluricus (Branson and Mehl), Panderodus unicostatus (Branson and Mehl).

4.1 The isotope δ13 C_{carb}

The isotopic characteristics of carbonates of the boundary Ludlow-Pridoli deposits in section 236 have shown that they are characterized by δ13Scarb values, in range from –7.9 to –1.8 ‰. Two intervals with sharp negative peaks δ13 C_{carb} in the section of the Upper Ludlow are distinguished on the isotope-carbon curve (*Fig.* 2).

The Pridoli part of the section is characterized by δ13 C_{carb} values from -3.6 to -0.6 ‰. In the lower part of the Pridoli, a sharp shift of the curve from negative values of δ13C_{carb} is recorded in the direction of positive values with an amplitude of oscillations of 3 ‰. Higher the values of δ13 C_{carb} are fairly constant. They are characterized by gradual weighting of the isotope δ13 C_{carb} to –1.0 ‰, which determines the trend of the positive direction of the curve. The values of this interval fall on the layers of limestones with characteristic lumpy detachment enclosing diverse fauna of Pridoli age (*Fig. 2*).

Thus, the curve of the isotope δ13 C_{carb} lies in the region of negative values of δ13 C_{carb} with two negative excursions. The sharp decreases of δ13 C_{carb} in the first and second interval (down to –7.9 ... –7.4) indicate significant changes in the characteristics of the sedimentation environment in Timan-Northern Urals marine basin.

Thus, the boundary Ludlow-Pridoli is determined by the contact of variegated clays and dolomites with large and lithoclasts (break breccias), above which dark gray lumpy limestones with interlayers of black carbonaceous and greenish-gray mudstones lie.

The major ecosystem restructuring associated with the Lower Pridolian Event is traced in sections in the North-East of Eurasia, the Arctic islands of Russia (Vaigach, N. Zemlya, Dolgiy) and Canada, Alaska [15, 16, 17, 18, 19].

5. Conclusions

The obtained results indicate the global character of the biotic rearrangements at the end of the Ludlow and at the very beginning of the Pridoli, the traces of which were preserved in the reference section of the Upper Silurian in the Subpolar Urals.

The decline in sea level, the widespread development of stromatolite-forming biota, the reduction of biodiversity, the disappearance of conodonts of the genus Adctenognathodus at the end of the Ludlow and the change in the dominants in the biota at the beginning of the Pridoli reflect the general response of organisms of different hierarchies (brachiopods, ostracods, conodontophorides and microbials) to habitat conditions late Ludlow and at the boundary Ludlow-Pridoli in Timan-Northern Urals marine paleobasin. The significant shallowing of Timan-Northern Urals marine basin at the end of Ludlow caused the death of a large mass of microbial communities, as well as abundant and diverse biota of the Ludlow reefs.

5. Acknowledgements

The authors are grateful to P. Männik for joint study of the section, T. Märss for the determination of vertebrate remains, A.V. Zhuravlev for valuable advice and comments, and to I.V. Smoleva, engineer of the Geonauka Center of the Institute of Geology of the Komi Science Center, Uralian Division of the Russian Academy of Sciences, for the determination of the isotope δ^{13} C_{carb} in carbonate rocks.

References

[1] Antsygin, N. Ya. (1994): Explanatory note to Ural stratigraphic maps. *Nauka Publishers*, Ekaterinburg, 95 p.

[2] Modzalevskaya, T. L. – Marss, T. (1991): On the age of the lower boundary of the Greben Regional Stage of the Urals. *Proceedings of the Estonian Academy of Sciences*. Geology. Vol. 40, No. 3, pp. 100–103.

[3] Puchkov, V. N. (2010): Geology of the Urals and Cis-Urals (actual problems of stratigraphy, tectonics, geodynamics and metallogeny). *Design Poligraph Service*, Ufa. 280 p.

[4] Yudin, V. V. (1994): Orogenez Severa Urala i Pay-Khoya. *Nauka Publishers,* Ekaterinburg. 286 p.

[5] Beznosova, T. M. (2008): Brachiopod communities and biostratigraphy of Upper Ordovician, Silurian and Lower Devonian of North-Eastern margin of Baltia paleocontinent. *Nauka Publishers*, Ekaterinburg, 218 p.

[6] Opornye razrezy verkhnego ordovika I nizhnego silur Pripolyarnogo Urala (Upper Ordovician and Silurian outcrops of Subpolar Ural). *Komi filial* AN SSSR, 1987, 34 p.

[7] Modzalevskaya, T. L. (1985): Silurian and the Early Devonian brachiopods from the European part of the USSR. *Order Atiridida*. M., 128 p.

[8] Matveev, V. A. – Kanev, B. I. (2016): Features of the upper Ludlow deposits in the Silurian key section on the western slope of the Subpolar Urals. *Vestnik of Institute of Geology of Komi SC UB RAS*. No. 8, pp. 3–8. https://doi.org.10.19110/2221-1381-2016-8-3-8

[9] Kanev, B. I. – Beznosova, T. M. – Matveev, V. A. – Gömze, L. A. (2017): Environment changes at the Ludlow and Pridoli boundary (Subpolar Urals). *Építőanyag – Journal of Silicate Based and Composite Materials,* Vol. 69, No. 4. pp. 132-133. https://doi.org./10.14382/epitoanyag-jsbcm.2017.24

[10] Beznosova, T. M. (2000) Silurian brachiopods in the Timan-norhtern Ural region: zonation and palaeoecology. *Proceedings of the Estonian Academy of Sciences*, Geology, Vol. 49, pp. 126–146.

[11] Abushik, A. (2000): Silurian–earliest Devonian ostracode biostratigrahy of the Timan-Norhtern Ural region, *Proceedings of the Estonian Academy of Sciences*, Geology, Vol. 49. pp. 126–146

[12] Beznosova, T. M. – Matveev, V. A. – Sokolova, L. V. – Kanev B. I. (2017): Regional manifestation of the global Ludford event (Lau Event) in the section of the Western slope of the Subpolar Urals. *Geodynamics, substance, ore genesis of the East European Platform and its folded framing: Extended abstract of scientific conference reports*. Syktyvkar: IG Komi SC UB RAS. pp. 19-21.

[13] Cherkesova, S. V. (1970): Silurian Greben stage of the island Vaigach. Stratigraphy and fauna of Silurian deposits of Vaigach. *Proceedings of the Scientific Research Institute of Geology of the Arctic*, pp. 4–24.

[14] Nikiforova, O. I. (1970): Brachiopods of Greiben stage of the island Vaigach (Late Silurian). Stratigraphy and fauna of Silurian deposits of Vaigach. *Proceedings of the Scientific Research Institute of Geology of the Arctic*, pp. 97-149.

[15] Baranov, V. V. – Blodgett, R. B. (2013): Correlation of the Pridolian beds (upper Silurian) of the Arctic regions of Eurasia and North America. *Otechestvennaya geologiya*. No. 5, pp. 52–57.

[16] Baranov, V. V (2015): Global events Lower Pridolsky and Klonk in the Middle Paleozoic in the northeast of Eurasia and in adjacent territories. *Nauka i obrazovaniye*. No. 3 (79). pp. 33–37.

[17] Jeppsson, L. (1998): Silurian oceanic events. A summary of general characteristics. In: Landing, E., Johnson, M.E. (Eds.), Silurian Cycles: Linkages of Dynamic Stratigraphy with Atmospheric, Oceanic and Tectonic Changes, *James Hall Centennial Volume*, New York State Museum Bulletin, Vol. 491, pp. 239–257.

[18] Jones, B. (1997): Variation in the upper Silurian brachiopod Atrypella phoca (Salter) from Somerset and Prince of Wales island, Arctic Canada. *Journal of Paleontology*, Vol. 51, No. 3, pp. 459–479.

[19] Nekhorosheva, L. V. – Patrunov, D. K. (1981): Greben stage of the Island Vaygach-Novaya Zemlya region. *Sovietskaya Geologiya*. No. 4, pp. 80–85.

Ref.:
Beznosova, Tatiana M. – **Matveev,** Vladimir A. – **Sokolova,** Lioubov V.: *Upper Ludlowian-lower Pridolian stratigraphy, carbon isotope of the Timan-Northern Urals region*
Építőanyag – Journal of Silicate Based and Composite Materials, Vol. 71, No. 1 (2019), 24–27. p.
https://doi.org/10.14382/epitoanyag-jsbcm.2019.5

Electrochemical study of Propolis as anti-oxidative reagent against to lead ions in rabbit blood samples using cyclic voltammetry

Muhammed Mizher RADHI ▪ Radiology, Health and Medical Technology College-Baghdad, Middle Technology University, Iraq ▪ mmradhi@yahoo.com
Bahaa Fakhri HUSSEIN ▪ College of Veterinary Medicine, University of Baghdad, Baghdad, Iraq
Ahmed Adeeb MOHAMED ▪ College of Veterinary Medicine, University of Baghdad, Baghdad, Iraq

Érkezett: 2018. 11. 16. ▪ Received: 16. 11. 2018. ▪ https://doi.org/10.14382/epitoanyag-jsbcm.2019.6

Abstract
One of the causes of autism disease is known to be the contamination of lead compounds for pregnant women or the children. The purpose of the research is to be proven the effect of lead ions by in vivo method on the samples of rabbit blood using cyclic voltammetric technique and to identify the effect of the antioxidant reagent namely propolis compound. The electrochemical analysis method was used in this study by cyclic voltammetric technique to determine the effect of propolis on the oxidation current peak of lead ions in blood medium (samples of rabbit blood). It was found that propolis compound acts as antioxidative reagent to reduce the oxidation current peak of lead ions to minimize value of current, it means that propolis compound is doing to eliminating the effect of lead ions in the blood and preventing it from precipitating the lead ions on the brain through the stream of blood in the animal body.
Keywords: lead ions, blood medium, cyclic voltammetry, GCE, propolis, autism, rabbit
Kulcsszavak: ólom ionok, vér közeg, ciklikus voltammetria, GCE, propolisz, autizmus, nyúl

Muhammed Mizher RADHI
Professor, Department of Radiological Techniques, Health and Medical Technology College-Baghdad, Middle Technical University, Baghdad, Iraq. He received his PhD from University Putra of Malaysia (UPM) at 2010 in Electrochemistry, Nanotechnology. Research topics: conductivity of grafted polymer with nano-deposit and fabrication of sensors by nanomaterials to study drugs in blood medium by electrochemical analysis.

Bahaa Fakhri HUSSEIN
Assistant Professor: anatomy and histology department, College of Veterinary Medicine, University of Baghdad, Baghdad, Iraq. He received his PhD from University Putra of Malaysia (UPM) at 2010 in bone tissue engineering. Research topics: tissue engineering and stem cells.

Ahmed Adeeb MOHAMED
PhD student in anatomy and histology, College of Veterinary Medicine, University of Baghdad, Iraq

1. Introduction

Many scientists have studied the effect of lead ions in different electrolytes such as blood medium to determine the oxidative effect of lead ion [1-5].

Propolis or bee glue is a resinous mixture that honey bees produce by mixing saliva and beeswax with exudate gathered from tree buds, sap flows, or other botanical sources [6,7]. Blood samples of rabbits were studied before and after given propolis during which clinical signs, body weight, mortality rate and histopathological changes associated with challenge of rabbits with *P. multocida* strain were recorded [8]. It is possible to prove protective roles of propolis against Pb-induced neurotoxicity. The results showed that co-administration of propolis with Pb inhibited Pb-induced neurological toxicity, as indicated by normalization of inhibition of brain MDA and PCC formation. Also, propolis protects the mitochondrial NADH-cytochrome C reductase, SDH and cytochrome C activities from Pb-induced amelioration. Furthermore, propolis increased vitamin C, vitamin E and P-SH levels in rat's brain. It can be concluded that propolis has beneficial effects and could be able to antagonize Pb-induced neurotoxicity [9]. Propolis has been attracting scientific attention since it has many biological and pharmacological properties, which are related to its chemical composition. Several *in vitro* and *in vivo* studies have been performed to characterize and understand the diverse bioactivities of propolis and its isolated compounds, as well as to evaluate and validate its potential. Yet, there is a lack of information concerning clinical effectiveness. The aim of this review is to discuss the potential of propolis for the development of new drugs by presenting published data concerning the chemical composition and the biological properties of this natural compound from different geographic origins [10]. Oxidative stress seems to play a very important role in the carcinogenic process. Reactive oxygen species (ROS) can elicit multiple effects by mediating carcinogen activation, causing DNA damage, and interfering with the repair machinery of the damaged DNA. In addition, ROS levels increases in preneoplastic cells during their promotion stage. This seems to induce the growth of initiated cells, and to play a role during cell cycle progression either by further damage the unstable genetic material or by altering the growth of tumor cells. Thus, tumor cells continually undergo high and persistent oxidative stress by ROS although this stress does not appear to be enough to induce cell death. On the contrary, as a hormetic effect, pleneoplastic cells show increased cell resistance to ROS because the cell antioxidant mechanisms are induced. Thus, they showed high levels of internal antioxidants such as coenzyme Q (CoQ) and are also able to accumulate high levels of ascorbate and reduced glutathione. These high levels of endogenous antioxidants may increase the chemotherapeutic resistance of the cells [11].

In this work, it was used a new method to prove that propolis compound can act as inhibition reagent for oxidation lead ions in the brain of rabbits.

2. Experimental

2.1 Materials

Groups of five 1.5-2 year old local breed rabbits (*Oryctolagus cuniculus*) weighting ~1.5kg were used. One group was injected intraperitoneally (IP) with 1 mg/kg lead acetate (Central Drug

House, Leiden, Netherlands) dissolved in distilled water and another injected lead but also and fed orally 750mg/kg propolis and deionized water for dilute the blood samples.

2.2 Apparatus

Instruments: EZstat series (potentiostat/glvanostat) NuVant Systems Inc. pioneering electrochemical technologies USA. Electrochemical workstations of Bioanalytical system with potetio-state driven by electroanalytical measuring software was connected to personal computer to perform cyclic voltammetry (CV), glassy carbon electrode (GCE), Ag/AgCl (3M NaCl) and Platinum wire (1 mm diameter) was used as a working, reference and counter electrode respectively. The surface of GCE was cleaned by polishing with alumina solution and about ten minutes in sonic water path to remove any impurities before using in the cell of CV.

2.3 Procedure

Each sample of rabbit blood (volume of 1 ml) was diluted with 9 ml of deionized water, the mixture placed in quartz cell of 10 ml, three electrodes (glassy carbon electrode as working electrode, Ag/AgCl as reference electrode and platinum wire as counter electrode) were immersed in the mixture of blood sample. The three electrodes were connected with potentiostat to determine the results by the cyclic voltammogram using personal computer [12].

3. Results and discussion

3.1 Effect lead ions on the blood components at different period weeks

Results are shown in *Table 1* and represented in *Figs. 1* and *2*. Electrochemical analysis of cyclic voltammetry of lead ion oxidation in blood produced a current peak of 400 mV with 8.64 uA in the 1st week after injection of rabbit with lead Pb(II). In those fed with propolis, the current reduced to 3.8 uA, a difference of (ΔIpa) about 4.84 uA. By the third to 8 period of testing the differences remained. By the 9th week we obtained a peak of 16.8 uA in that had been exposed to lead where in that propolis, voltage reduced to 3.53 uA a difference of 13.27 uA. The findings suggest that propolis may have reduce oxidation by lead ions in blood [13, 14].

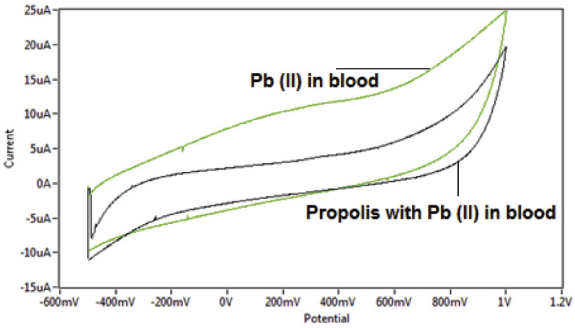

Fig. 1. Cyclic voltammograms measured in rabbit blood with lead ions or propolis (with lead ions as well) during the first week of tests; GCE as working electrode versus Ag/AgCl (3M NaCl) as reference electrode.

1. ábra Ciklikus voltammogramok; nyúl vér minták ólom tartalommal, propolisszal etetve vagy anélkül, a vizsgálatok első hetében; mérő elektróda: GCE, referencia elektróda: Ag/AgCl (3M NaCl).

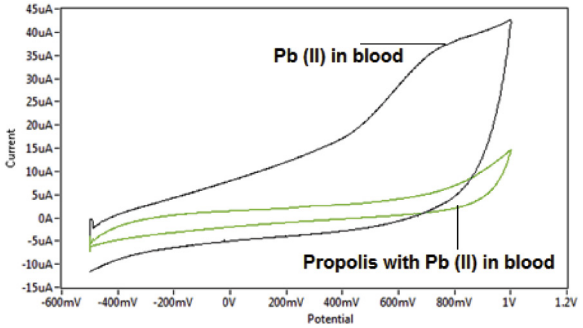

Fig. 2. Cyclic voltammograms measured in rabbit blood with lead ions or propolis (with lead ions as well) during the 9th week of tests; GCE as working electrode versus Ag/AgCl (3M NaCl) as reference electrode.

2. ábra Ciklikus voltammogramok; nyúl vér minták ólom tartalommal, propolisszal etetve vagy anélkül, a vizsgálatok kilencedik hetében; mérő elektróda: GCE, referencia elektróda: Ag/AgCl (3M NaCl).

	Ipa (uA)	ΔIpa (reducing)	Concentration (mM)	Concentration (mg)
period (1) 20-3-2017				
Pb + blood	8.64		0.008	3.035
Pb + blood +Propolis	3.8	4.84	0.0013	0.493
period (2) 26-3-2017				
Pb + blood	11.5		0.015	5.69
Pb + blood +Propolis	3.98	7.52	0.0014	0.531
period(3) 2-4-2017				
Pb + blood	12.7		0.021	7.966
Pb + blood + Propolis	3.43	8.27	0.0011	0.417
period (4) 9-4-2017				
Pb+blood	14.5		0.025	9.483
Pb + blood + Propolis	2.73	11.77	0.00094	
period (5) 17-4-2017				
Pb+blood	12.7		0.02	7.966
Pb + blood + Propolis	2.28	10.42	0.0009	0.341
period (6) 24-4-2017				
Pb + blood	14.8		0.027	10.242
Pb+ blood+ Propolis	2.84	11.96	0.00096	0.364
period (7) 30-4-2017				
Pb+blood	15.2		0.029	11
Pb+blood+Propolis	2.49	12.71	0.00093	0.353
period (8) 7-5-2017				
Pb + blood	19.2		0.039	14.793
Pb+blood+Propolis	4.02	15.18	0.0014	0.531
period(9) 14-5-2017				
Pb+blood	16.8		0.032	12.138
Pb+blood+Propolis	3.53	13.27	0.0011	0.417

Table 1. Oxidation current peak and concentration of lead ions in rabbit blood exposed to lead ions or fed propolis (with lead ions)

1. táblázat Oxidációs csúcs áramerősségek és ólom ion koncentráció nyúl vér mintákban ólom tartalommal, propolisszal etetve vagy anélkül

3.2 Effect the concentration of Pb(II) in blood samples before and after feeding omega 3 fatty acid on the rabbit

Lead ions in blood were measured by cyclic voltammetry. One group of 5 rabbits was injected 1mg/kg lead acetate dissolved in distilled water. Another group of 5 rabbits were injected 1mg/kg lead acetate IP but also fed 750mg/kg propolis. A plot of lead concentration in blood versus time shows that

lead concentrations increased over time with a correlation of R^2=0.85 as shown in *Fig 3*. In those given propolis with lead the concentration of lead declined over time as shown in *Fig. 4* as reported by others [15-17].

In vivo study of rabbit blood samples have been searched by electrochemical method using cyclic voltammetric technique to find the effect of presence of lead ions in the blood samples which received from injected rabbit with Pb((II), other blood samples were received from rabbit feeding with propolis after injected with Pb(II) dose. Both samples were studied to find the effect of oxidant reagent (lead ions) and antioxidant reagent (propolis) on blood component. It was found the concentration of lead ions in blood sample was increased against to period week as shown in *Table 1* and *Fig. 3*. A good sensitivity was calculated from the relationship in the *Fig. 3* is equal to 0.85. On the other hand, the concentration of lead ions in blood sample of feeding rabbit with propolis was decreased as shown in *Table 1* and *Fig. 4*. It means that omega compound was affected on the lead ions in blood medium which act inhibition of oxidative effect, so omega works to reduce lead action on the blood components [18-20].

It can be said that any blood contaminated with lead ions causes atrophy in the brain, this leads to symptoms of Alzheimer›s disease in the adults or autism disease in children [21-23]. But, it was found that propolis was stopped the negative effective of lead ions especially in brain.

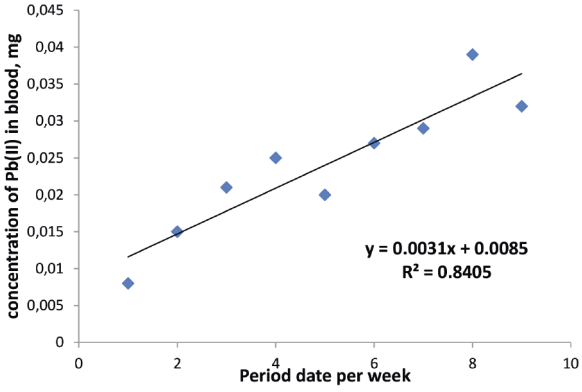

Fig. 3. Lead (mg) in blood of rabbit (injected lead) against time (weeks)
3. ábra Ólom (mg) nyúl vérben (injekciózott ólom) az idő függvényében

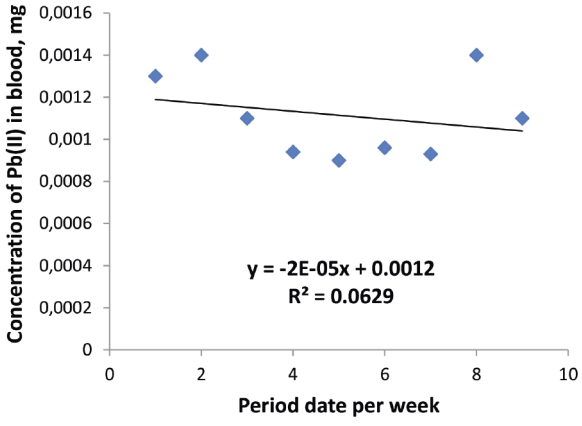

Fig. 4. Lead (mg) in blood of rabbits fed propolis against time (weeks)
4. ábra Ólom (mg) nyúl vérben (propolisszal etetve) az idő függvényében

4. Conclusion

The study was included to find the effect of lead ions on the brain of group of rabbits by electrochemical method, also to prove the effect of propolis on the brain of contaminate rabbit with lead ions, it was found the propolis acts as antioxidative reagent which decrease and inhibited effect of lead on the brain of rabbit, so we can said any contamination with lead ions was treated with propolis to stop the oxidation effect of lead ions in blood medium of rabbits.

It can be getting an important conclusion from this research so as to the importance of the special theme of the new diseases such as autism and Alzheimer. It has been studied the blood samples from rabbits exposure to contamination to the lead ions using electrochemical analysis by cyclic voltammetric method, the results show high anodic current peak at 400 mV for the Pb(II) in the blood samples and this peak was increased against to increasing the dose of Pb(II) through nine weeks. But the surprise in the results of the analysis for blood samples which received from the rabbit injected with Pb(II) and feeding with propolis that the oxidation current peak of lead ion was reduced from 8.64 uA to 3.8 uA, this mean the concentration of lead ions was reduced from 12.138 mg/L to 0.417 mg/L in blood samples. Propolis is one of the most antioxidants acts to inhibition the activity of Pb(II) in blood medium. So, it can be said that some diseases causes by the contamination with lead ions can be treated with propolis.

References

[1] Mehta, P. (2012): Cyclic Voltammetric Study of Lead (Pb(II)) in Different Potassium Salts as Supporting Electrolytes, *International Journal of Pure Applied Chemistry*, Vol. 7, No. 2, pp. 14-21.

[2] Radhi, M. M. – Albakry, A. A. A. – Jassim, A. M. – Alassady, S. A. – Al-Mulla, E. A. J. (2016): Electrochemical Study of Pb(II) in Present of Each Ascorbic Acid, Glucose, Urea and Uric Acid Using Blood Medium as an Electrolyte, *Nano Biomedicine and Engineering*, Vol. 8, No. 1, pp. 9-15. https://doi.org.10.5101/nbe.v8i1.p9-15

[3] Radhi, M. M. – Abdullah, H. N. – Jabir, M. S. – Al-Mulla, E. A. J. (2017): Electrochemical Effect of Ascorbic Acid on Redox Current Peaks of $CoCl_2$ in Blood Medium, *Nano Biomedicine and Engineering*, Vol. 9, No. 2, pp. 103-106. https://doi.org.10.5101/nbe.v9i2.p103-106

[4] Radhi, M. M. (2017): Voltammetric Study of the Redox Current Peaks of Pb(II) Mediated by GCE in Normal Saline, *American Journal of Chemical and Biochemical Engineering*, Vol. 2, No. 2, pp. 26-34. https://doi.org.10.11648/j.ejb.20170503.11

[5] Radhi, M. M. – Hussein, B. F. – Mohamed, A. A. (2018): Effect of Omega 3 fatty acid on lead ion anodic current peak in blood of rabbits measured by cyclic voltammetry, *Online Journal of Veterinary Research*, Vol. 22, No. 1, pp. 1-6, 2018.

[6] Scheller, S. – Szaflarski, J. – Tustanowski, J. – Nolewajka, E. – Stojko, A. (1977): Biological properties and clinical application of propolis. I. Some physico-chemical properties of propolis, *Arzneimittel-Forschung*, Vol. 27, No. 4, pp. 889-890.

[7] Marín, D. – García, P. (2008): New research on antioxidants, *Nova Biomedical Books*, New York, 2008.

[8] Nassar, S. A. – Mohamed, A. H. – Soufy, H. – Nasr, S. M. (2013): Protective Effect of Egyptian Propolis against Rabbit Pasteurellosis, *BioMed Research International*, Volume 2013, Article ID 163724, 9 pages https://doi.org/10.1155/2013/163724

[9] El-Masry, T. A. – Emara, A. M. – El-Shitany, N. A. (2011): Possible protective effect of propolis against lead induced neurotoxicity in animal model, *Journal of Evolutionary Biology Research*, Vol. 3, No. 1, pp. 4-11.

[10] Mizrahi, A. – Lensky, Y. (1997): Bee Products: Properties, Applications, and Apitherapy, *Springer Science, Business Media, LLC*, 1997.

[11] Silva-Carvalho, R. – Baltazar, F. – Almeida-Aguiar, C. (2015): Propolis: A Complex Natural Product with a Plethora of Biological Activities That Can Be Explored for Drug Development, *Evidence Based Complementary Alternative Medicine*. 2015: 206439 https://doi.org/10.1155/2015/206439

[12] Kilmartin, P. A. – Zou, H. – Waterhouse, A. L. (2001): A cyclic voltammetry method suitable for characterizing antioxidant properties of wine and wine phenolics. *Journal of agricultural and food chemistry,* Vol. 49, No. 4, pp. 1957-1965. https://doi.org/10.1021/jf001044u

[13] Abdel-Moneim, A. E. – Dkhil, M. A. – Al-Quraishy, S. (2011): The redox status in rats treated with flaxseed oil and lead-induced hepatotoxicity, *Biological Trace Element Research,* Vol. 143, No. 1, pp. 457–467. https://doi.org/10.1007/s12011-010-8882-z

[14] Elelaimy, I. A. – Elfiky, S. A. – Hassan, A. M. – Ibrahim, H. M. – Elsayad, R. I. (2012): Genotoxicity of anticancer drug Azathioprine (Imuran): role of omega-3 (ω-3) oil as protective agent, *Journal of Applied Pharmaceutical Science,* Vol. 2, No. 4, pp. 14–23. https://doi.org/10.7324/JAPS.2012.2404

[15] Murphy, M. E. P. – Brayer, G. D. – Fetrow, J. S. – Burton, R. E. (1993): The structure and function of omega loop A replacements in cytochrome c. *Chemistry, Physics, Polymers & Materials Science,* Vol. 2, No. 9, pp. 1429–1440. https://doi.org/10.1002/pro.5560020907

[16] Ashton Acton, Q. (2011): Advances in Biotechnology Research and Application: 2011, Amazon.com., USA.

[17] Crespi, B. – Stead, P. – Elliot, M. (2010): Evolution in health and medicine Sackler colloquium: Comparative genomics of autism and schizophrenia. *Proceedings of the National Academy of Sciences of the United States of America.* Vol. 107, No. 1, pp. 1736–41. https://doi.org/10.1073/pnas.0906080106

[18] Szpir, M. (2006): Tracing the origins of autism: a spectrum of new studies. *Environmental Health Perspectives.* Vol. 114, No. 7, pp. A412–8. https://dx.doi.org/10.1289%2Fehp.114-a412

[19] Burns, A. – Iliffe, S. (2009): Alzheimer›s disease. *The BMJ.* Vol. 338, b158. https://doi.org/10.1136/bmj.b158

[20] Querfurth, H. W. – LaFerla, F. M. (2010): Alzheimer›s disease. *The New England Journal of Medicine.* Vol. 362, No. 4, pp. 329–44. https://doi.org/10.1056/NEJMra0909142

[21] Caronna, E. B. – Milunsky, J. M. – Tager-Flusberg, H. (2008): Autism spectrum disorders: clinical and research frontiers. Arch Dis Child. 2008; Vol. 93, No. 6, pp. 518–23. https://doi.org/10.1136/adc.2006.115337

Ref.:
Radhi, Muhammed Mizher – **Hussein,** Bahaa Fakhri – **Mohamed,** Ahmed Adeeb: *Electrochemical study of Propolis as anti-oxidative reagent against to lead ions in rabbit blood samples using cyclic voltammetry*
Építőanyag – Journal of Silicate Based and Composite Materials, Vol. 71, No. 1 (2019), 28–31. p.
https://doi.org/10.14382/epitoanyag-jsbcm.2019.6

GUIDELINE FOR AUTHORS

The manuscript must contain the followings: title; author's name, workplace, e-mail address; abstract, keywords; main text; acknowledgement (optional)**; references; figures, photos with notes; tables with notes; short biography** (information on the scientific works of the authors).

The full manuscript should not be more than 6 pages including figures, photos and tables. Settings of the word document are: 3 cm margin up and down, 2,5 cm margin left and right. Paper size: A4. Letter size 10 pt, type: Times New Roman. Lines: simple, justified.

TITLE, AUTHOR

The title of the article should be short and objective.

Under the title the name of the author(s), workplace, e-mail address.

If the text originally was a presentation or poster at a conference, it should be marked.

ABSTRACT, KEYWORDS

The abstract is a short summary of the manuscript, about a half page size. The author should give keywords to the text, which are the most important elements of the article.

MAIN TEXT

Contains: materials and experimental procedure (or something similar), results and discussion (or something similar), conclusions.

REFERENCES

References are marked with numbers, e.g. [6], and a bibliography is made by the reference's order. References should be provided together with the DOI if available.

Examples:

Journals:

[6] Mohamed, K. R. – El-Rashidy, Z. M. – Salama, A. A.: In vitro properties of nano-hydroxyapatite/chitosan biocomposites. *Ceramics International.* 37(8), December 2011, pp. 3265–3271, http://doi.org/10.1016/j.ceramint.2011.05.121

Books:

[6] Mehta, P. K. – Monteiro, P. J. M.: Concrete. Microstructure, properties, and materials. *McGraw-Hill*, 2006, 659 p.

FIGURES, TABLES

All drawings, diagrams and photos are figures. The **text should contain references to all figures and tables**. This shows the place of the figure in the text. Please send all the figures in attached files, and not as a part of the text. **All figures and tables should have a title**.

Authors are asked to submit color figures by submission. Black and white figures are suggested to be avoided, however, acceptable.

The figures should be: tiff, jpg or eps files, 300 dpi at least, photos are 600 dpi at least.

BIOGRAPHY

Max. 500 character size professional biography of the author(s).

CHECKING

The editing board checks the articles and informs the authors about suggested modifications. Since the author is responsible for the content of the article, the author is not liable to accept them.

CONTACT

Please send the manuscript in electronic format to the following e-mail address: femgomze@uni-miskolc.hu and epitoanyag@szte.org.hu or by post: Scientific Society of the Silicate Industry, Budapest, Bécsi út 122–124., H-1034, HUNGARY

We kindly ask the authors to give their e-mail address and phone number on behalf of the quick conciliation.

Építőanyag – *Journal of Silicate Based and Composite Materials*, Quarterly peer-reviewed periodical of the Hungarian Scientific Society of the Silicate Industry, SZTE.
http://epitoanyag.org.hu

Precursor-BioBased

Developing novel precursor fibre (PF) materials from blends of modified lignin and biopolymers which can be converted to carbon fibre (CF) using industry standard heating processes so that current manufacturing plant can continue to be used.

Energy efficient / cost reduction

Reducing energy consumption, including CO2 emissions, associated with the traditional manufacture of CF through the development of new low energy, cost effective biobased PF to CF conversion technologies.

Carbon Fibre

Establishing a new value chain for lignin by utilising low commercial value material to produce CF which will in turn be processed into carbon fibre reinforced polymers (CFRP).

Composites

Enabling EU based companies to build a technological lead and competitive advantage through the establishment of an indigenous capability to manufacture carbon fibre from sustainable precursors using energy efficient and cost-effective technology; this is of paramount importance for European competitiveness in the composites market.

libre2020.eu

Euromines is the recognised representative of the European metals and minerals mining industry. The association's main objective is to promote the industry and to maintain its relations with European institutions at all levels. Euromines provides services to its members with regard to EU policy and serves as a network for cooperation and for the exchange of information throughout the sector within Europe. The association also fosters contacts with the mining community throughout the world.

Euromines represents large and small companies and subsidiaries in Europe and in other parts of the world which provide jobs to more than 350,000 people. Through the activities and operations of these members, more than 42 different metals and minerals are produced. For some metals and minerals, Europe is the world's leading producer.

Euromines provides a formal platform in which the members evaluate the impact of European and International policies and legislation on the industry and define common positions and actions.

www.euromines.org